scientific reports

Check for updates

OPEN

Elevated serotonin receptor 2A signaling restores learning and memory in a Fragile X syndrome model

Yuchen Du[1], Vanessa K. Miller[1], Andrew J. Mellies[1] & Kendal Broadie[1,2,3,4,5]✉

Serotonin (5-hydroxytryptamine, 5-HT) has central roles enabling learning and memory, particularly via serotonin receptor 2A (5-HT$_{2A}$R) signaling. *Drosophila* Fragile X syndrome model (*dfmr1* null mutant) studies reveal impaired learning and memory, which may reflect serotonergic signaling deficits. Here, we use classical olfactory T-maze conditioning to assess behavior, combined with imaging to assess 5-HT and 5-HT$_{2A}$R levels within the underlying Mushroom Body (MB) brain circuitry. Null *dfmr1* mutants exhibit learning and memory deficits that are corrected by elevating 5-HT signaling via 1) overexpression of the serotonin biosynthetic enzyme tryptophan hydroxylase (Trhn) or 2) knockdown of the serotonin reuptake transporter (SERT). Direct comparisons reveal both Trhn and SERT manipulations equally restore learning and memory in *dfmr1* null mutants. 5-HT$_{2A}$R levels in the MB circuit are reduced relative to controls in *dfmr1* mutants, and 5-HT$_{2A}$R RNAi phenocopies *dfmr1* null behavioral deficits, suggesting these phenotypes are primarily caused by the loss of 5-HT$_{2A}$R signaling. Consistently, 5-HT$_{2A}$R overexpression in *dfmr1* nulls restores normal learning and memory compared to controls. These findings suggest loss of 5-HT$_{2A}$R signaling causes learning and memory deficits in this Fragile X syndrome model, and that rectifying this signaling impairment can restore learning and memory, providing a framework for serotonergic intervention strategies.

Keywords Tryptophan hydroxylase, 5-hydroxytryptamine, Serotonin reuptake transporter, 5-HT$_{2A}$ receptor, Mushroom body, *Drosophila*

Fragile X syndrome (FXS) is the leading monogenetic intellectual disability (ID)[1,2], caused predominantly by epigenetic loss of the Fragile X Messenger Ribonucleoprotein (FMRP)[3,4]. Like human FXS patients, the well-established *Drosophila* FXS disease model[5,6] displays impairments in learning and memory[7,8], with defects in underlying brain Mushroom Body (MB) learning/memory circuitry[9,10] and dysfunction in multiple characterized molecular mechanisms[11–13]. This multifaceted FXS disease state may reflect truly independent FMRP functions, or could be interconnected via common foundational signaling nodes[14]. One intriguing possibility is that fundamental neuromodulator systems might compensate for impaired FXS learning/memory function[15]. Systematic brain proteomic analyses employing the *Drosophila* FXS model identified altered monoamine signaling pathways[16] utilizing serotonin (5-hydroxytryptamine,5-HT[17,18]. We hypothesized transgenic manipulation of serotonergic signaling could prove an effective compensatory method for the treatment of learning and memory behavioral impairments in the Fragile X syndrome disease condition.

Serotonin/5-HT is a key regulator of mammalian learning and memory[19–21]. Likewise, *Drosophila* serotonergic signaling regulates learning and memory, including courtship and aversive olfactory conditioning behaviors[22,23]. The MB circuit underlying olfactory learning and memory[24,25] receives serotonergic input and expresses conserved components of the serotonergic pathway, including 5-HT biosynthetic enzyme tryptophan hydroxylase (Trhn) and the serotonin transporter (SERT)[26–29]. Importantly, Trhn produces serotonin in neurons and glia in *Drosophila*[30]. Serotonin levels are upregulated in both FXS patients and disease models[16,18], although this is likely compensatory as selective serotonin reuptake inhibitor (SSRI) use improves FXS symptoms[31,32]. The serotonergic 5-HT$_{2A}$ receptor (5-HT$_{2A}$R) helps mediate mammalian learning and memory[21,33]. *Drosophila*

[1]Departments of Biological Sciences, Vanderbilt University and Medical Center, Nashville, TN 37235, USA. [2]Cell and Developmental Biology, Vanderbilt University and Medical Center, Nashville, TN 37235, USA. [3]Pharmacology, Vanderbilt University and Medical Center, Nashville, TN 37235, USA. [4]Kennedy Center for Research on Human Development, Vanderbilt University and Medical Center, Nashville, TN 37235, USA. [5]Vanderbilt Brain Institute, Vanderbilt University and Medical Center, Nashville, TN 37235, USA. ✉email: kendal.broadie@vanderbilt.edu

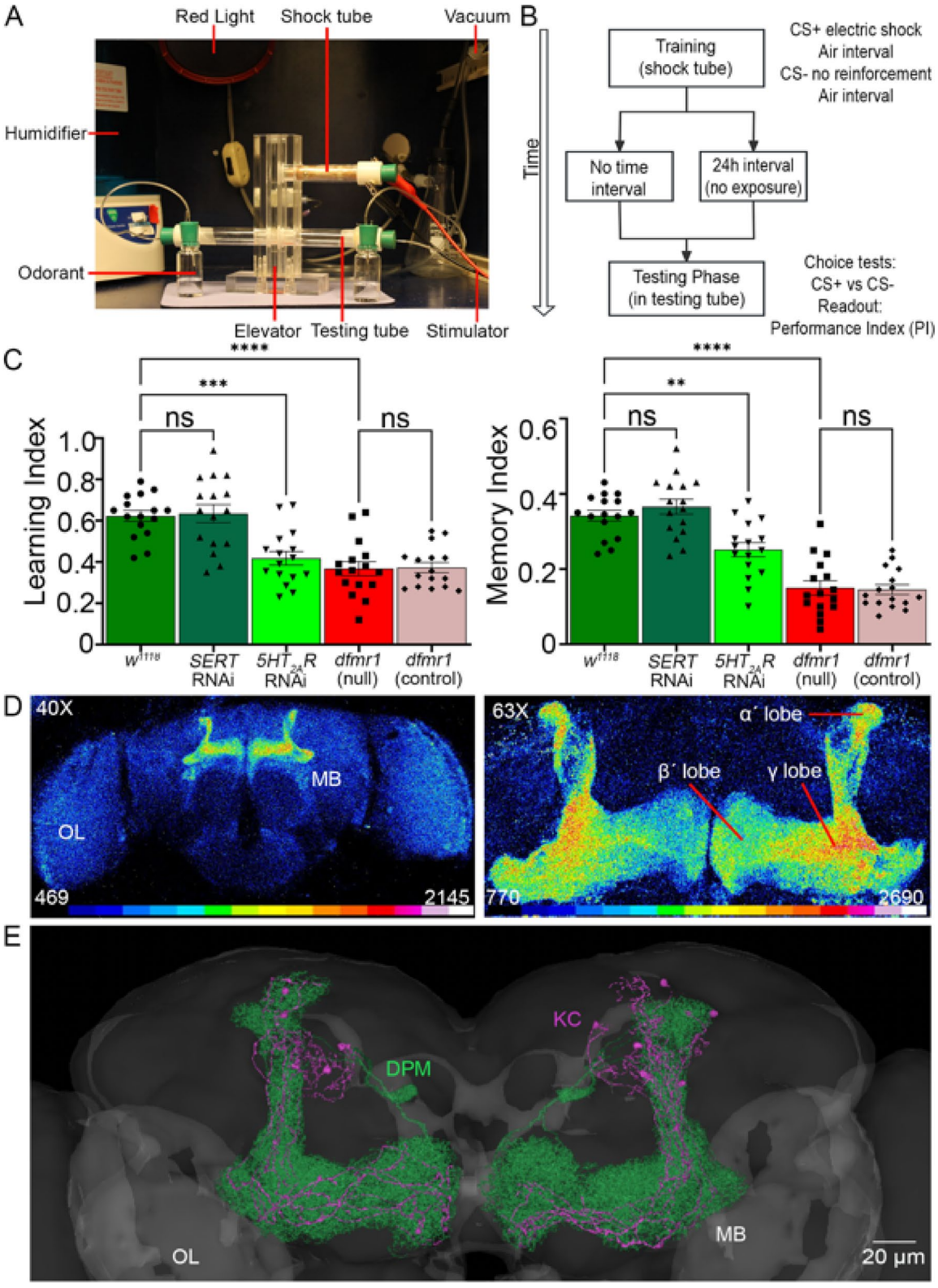

5-HT_{2A}Rs in neurons and glia function in olfactory circuitry[34], but olfactory learning/memory roles have not been tested. Nothing is known about 5-HT_{2A}R signaling in the *Drosophila* FXS model[35], although 5-HT_{2A}R signaling is altered in the mouse FXS model[36], with 5-HT_{2A}R proposed as a potential therapeutic target[17,18]. We hypothesized 5-HT_{2A}R signaling regulates normal learning and memory, and may be impaired in the FXS condition.

Here, we employ the *Drosophila* FXS model (*dfmr1* null mutants) to systematically investigate the contributions of serotonergic signaling to learning and memory, using classic aversive olfactory conditioning coupled to MB imaging of 5-HT and 5-HT_{2A}Rs. We designed experiments to probe serotonin signaling at three

◀**Fig. 1**. Learning and memory regulation via Mushroom Body serotonin signaling. (**A**) Aversive olfactory conditioning apparatus used for Pavlovian learning/memory assays. The setup includes red light illumination, humidity control, vacuum airflow odorant delivery, copper-grid shock tube with electrical stimulator (training), a vertical elevator for animal delivery, and a T-maze with two choice tubes (testing). Animals are trained with odorant cues paired to electric shock in the shock tube, and then scored in the T-maze test tubes. (**B**) Schematic flowchart of the learning and memory assays. The conditioning consists of alternating exposures to CS + odor paired with 12 shocks (80 V, 1.5 s duration, 5 s interval), air interval, and then the CS- odor without shock, followed by either immediate or delayed (24 h) T-maze testing. Across independent trials, OCT and MCH were assigned as CS^+ and CS^- in alternative experiments. Performance index ($PI = (CS^- - CS^+)/(CS^- + CS^+)$) reports learning/memory abilities. (**C**) Quantification of learning (left) and memory (right) PIs in 5 genotypes shown: genetic background control (w^{1118}); global *UH1*-Gal4 serotonin transporter (SERT) and serotonin receptor 2A ($5HT_{2A}R$) RNAi; FXS disease model (*dfmr1* null mutant) alone and with *UH1*-Gal4/ + (*dfmr1* control). Data show individual trials (n = 16/genotype), mean ± SEM, and one-way ANOVA with Tukey's multiple comparisons tests. For learning (left), there is a significant effect of genotype ($F(4,75) = 16.54$), with no significant difference between w^{1118} and *SERT* RNAi ($p = 0.9999$), while $5HT_{2A}R$ RNAi ($p = 2.588 \times 10^{-4}$) and *dfmr1* null mutants ($p = 1.924 \times 10^{-6}$) show reduced performance, with the *dfmr1* transgenic control not significantly different ($p = 0.9999$). For memory, there is a significant effect of genotype ($F(4, 75) = 36.21$), with no significant difference between w^{1118} and *SERT* RNAi ($p = 0.9759$), whereas $5HT_{2A}R$ RNAi ($p = 6.347 \times 10^{-3}$) and *dfmr1* null mutants ($p = 3.0 \times 10^{-11}$) show decreased performance. Again, *dfmr1* null and *dfmr1* control are not significantly different ($p = 0.9999$). The significance is indicated as $p > 0.05$ (not significant; ns), $p < 0.01$ (**), $p < 0.001$ (***), and $p < 0.0001$ (****). (**D**) *Drosophila* brain confocal images labeled with anti-Trio to reveal the Mushroom Body. Left: Whole-brain at 40 × magnification shows Mushroom Body (MB) and optic lobes (OL). Right: Higher magnification at 63 × showing MB α′, β′, and γ lobes. Fluorescence intensity is shown on a 16-color LUT scale. (**E**) Serotonergic innervation of the MB in an anatomical reconstruction from FlyWire codex. Dorsal paired medial neurons (DPM, green) provide serotonergic input onto MB Kenyon cells (KC, magenta; small subset shown for clarity).

levels: serotonin synthesis (Trhn), serotonin uptake (SERT), and serotonin receptor ($5\text{-}HT_{2A}R$) involvement. First, we manipulated serotonin/5-HT synthesis and reuptake using two cell-targeted transgenic methods: Trhn biosynthetic enzyme overexpression (OE) and SERT knockdown (RNAi). These complementary approaches test whether elevating serotonin alters learning and memory, and could compensate for *dfmr1* null mutant deficits. Second, $5\text{-}HT_{2A}$ receptors were similarly manipulated with cell-targeted $5\text{-}HT_{2A}R$ OE and RNAi. By manipulating the $5\text{-}HT_{2A}R$ levels, we aimed to determine whether $5\text{-}HT_{2A}$ receptor signaling is necessary and sufficient for normal learning/memory behavior, or could improve outcomes in the FXS model. We used classical olfactory conditioning to evaluate the effects of these serotonergic manipulations on associative learning and memory, paired to MB confocal imaging to quantify 5-HT and $5\text{-}HT_{2A}R$ levels. This combinatory approach allows us to link neuromodulatory ligand-receptor circuit signaling to cognitive behavioral output. Our goal was to determine whether targeted serotonergic interventions could restore learning and memory in the *Drosophila* FXS genetic disease model and to determine whether $5\text{-}HT_{2A}$ receptor signaling contributes to learning and memory rescue in this FXS model.

Methods

Drosophila genetics

All stocks fed standard *Drosophila* food were reared at 25 °C in humidified incubators on a 12:12-h light/dark cycle. Adults of both sexes staged to 7–9 days post-eclosion (dpe) were used in all studies. All stocks were backcrossed to the w^{1118} background, which was used as the genetic background control. For the Fragile X syndrome (FXS) disease model, the $dfmr1^{\Delta 50M}$ excision deletion null allele[6,37] was used in combination with multiple Gal4 drivers and UAS responder lines. The Gal4 driver lines were: ubiquitous *daughterless UH1*-Gal4 (RRID: BDSC 55850)[38], neuron-specific *elav*-Gal4 (RRID: BDSC 8765)[39], and glia-specific *repo*-Gal4 (RRID: BDSC 7415)[40]. The UAS responder lines were: a wildtype overexpression (OE) UAS-*Trhn* line (RRID: BDSC 27638)[41], UAS-*SERT* RNAi (RRID: VDRC 11346)[42], UAS-$5HT_{2A}R^{OE}$ (RRID: BDSC 4830), and UAS-$5HT_{2A}R$ RNAi (RRID: VDRC 31882)[43]. Transgenic combinations were generated using standard *Drosophila* genetic techniques. The control lines used were: (1) genetic background w^{1118} (RRID: BDSC 3605), (2) w^{1118};$Trhn^{OE}$/+; *UH1*-Gal4/ +, (3) w^{1118}; *SERT* RNAi/+; *UH1*-Gal4/+, (4) w^{1118}; $5HT_{2A}R$ RNAi/+; *UH1*-Gal4/+, and (5) w^{1118}; $dfmr1^{\Delta 50M}$; *UH1*-Gal4/ +. Experimental and control studies were always conducted in parallel for all behavioral and imaging analyses.

Behavioral analyses

Aversive olfactory conditioning was used to assess associative learning and memory, as previously described[8,44]. Briefly,In every trial, ~ 100 adults (7–9 days dpe) were tested for odorant conditioning behavior using a T-maze training and testing apparatus (Fig. 1A). All behavioral studies were performed in mixed sex cohorts, with the number of animals per replicate reported in Supplementary Table 1. 16 independent biological replicates were tested for each genotype and condition, with ~ 100 combined males and females per replicate (Table S1). The odorant conditioned stimulus (CS^+) was paired to electric shock in a copper grid training tube, followed by exposure to the unconditioned odorant (CS^-; Fig. 1B). Odorant solutions (9 µL in 8 mL mineral oil) were prepared fresh for each trial, balanced for equal aversiveness. In each individual training phase (12 trains of shock-training), a 60 s exposure to the CS^+ (alternately 3-octanol [OCT] or 4-methylcyclohexanol [MCH]) was

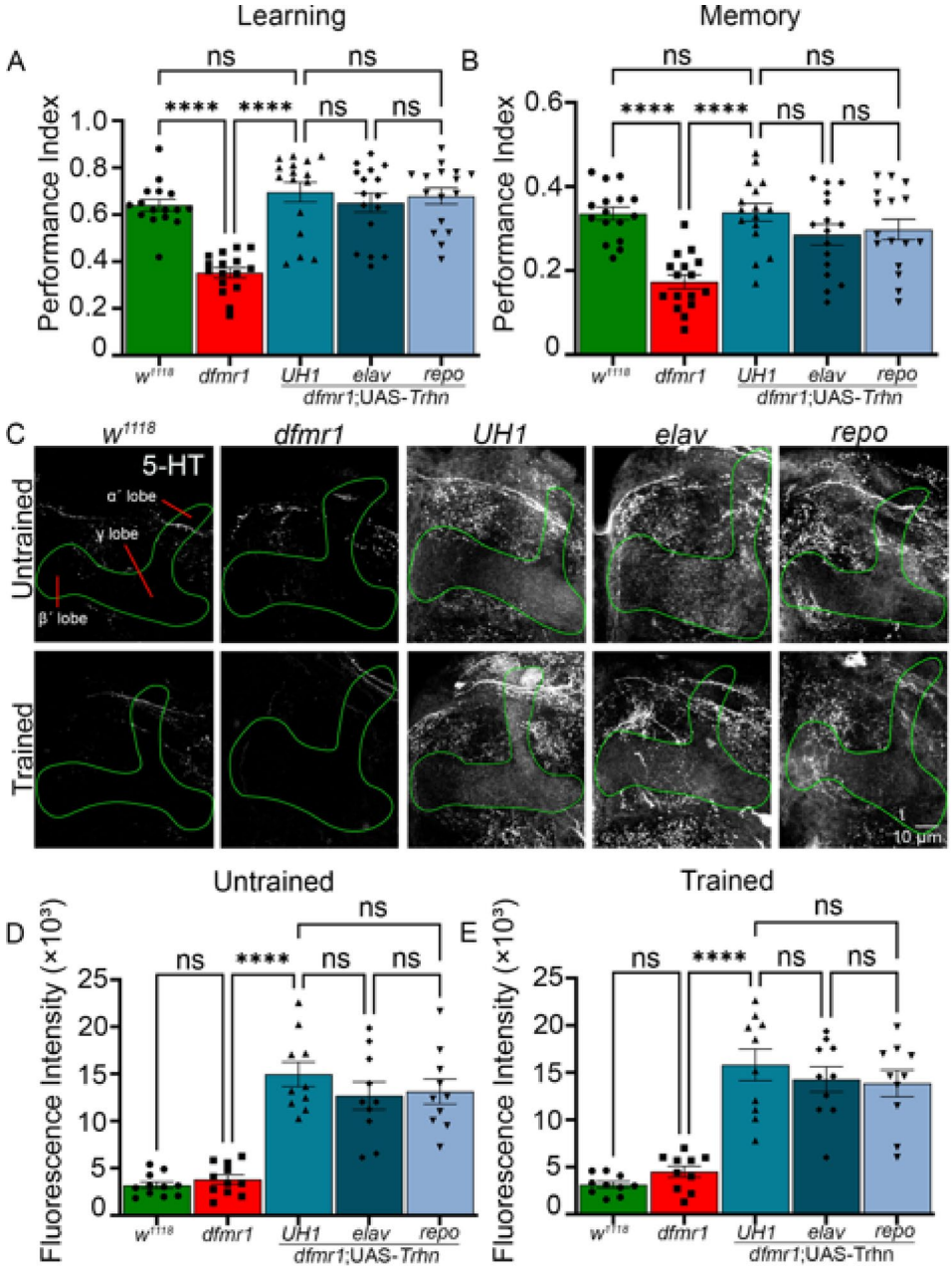

paired with electrical shock (1.5-s 80 V trains at 5-s intervals), then a 60 s air rest period, followed by another 60 s exposure to the CS^- odorant (opposing OCT or MCH) without electrical shock[44]. Immediately following training, animals were transferred within the T-maze using a central elevator (Fig. 1A,B) to test immediate odorant-shock association (defined as "learning"). Following memory training, animals were returned to food vials for a 24-h rest period and then re-introduced into the same T-maze (Fig. 1A,B) to test maintained odorant-shock association (defined as "memory"). For both trials, a 2 min period allowed choice between tubes containing CS^+ and CS^- odorants. Tubes were closed, animals anesthetized using CO_2, and then performance index (PI) was calculated blind to all genotypes using the formula: PI = CS^- tube number—CS^+ tube number/total animal number. The T-maze direction and odorants (OCT or MCH) used as CS^+ versus CS^- were reversed between every experiment to control for any bias.

Immunocytochemistry imaging

Mushroom Body (MB) antibody labeling and confocal imaging was done as previously described[5]. Briefly,Adults (7–9 dpe) were anesthetized in 70% ethanol for 1 min and then brains were dissected using sharpened forceps (Dumont #5) in 1 × phosphate-buffered saline (PBS; Invitrogen). Brains were fixed for 30 min at room temperature (RT) in 4% paraformaldehyde (PFA; EMS 15714) + 4% sucrose in PBS. The fixed brains were washed 3 × with PBS and then blocked for 1.5 h at RT with 1% bovine serum albumin (BSA; Sigma-Aldrich) + 0.2% Triton X-100 in PBS (PBS-T; Fisher Chemical). Brains were then incubated with primary antibodies + 0.2% BSA in PBS-T at 4 °C overnight. Primary antibodies used: rabbit anti-5-HT (Immunostar, 20,080 1:1,000), rabbit anti-$5HT_{2A}$R (Abcam, ab140524, 1:100), and mouse anti-Trio (Developmental Studies Hybridoma Bank (DSHB), 9.4A, 1:100).

◀**Fig. 2**. Tryptophan hydroxylase overexpression rectifies FXS learning/memory. Performance index quantification of learning (**A**) and memory (**B**) across five genotypes; genetic background control (w^{1118}; green), FXS model (*dfmr1*; red), and UAS-*tryptophan hydroxylase* (*Trhn*) overexpression in the *dfmr1* background driven by *UH1-* (ubiquitous), *elav-* (neuronal), and *repo-* (glial) Gal4 lines (blue). Data show individual trials (n = 16 each), mean ± SEM, and one-way ANOVA with Tukey's multiple comparisons tests. Learning performance shows a significant effect of genotype ($F(4,75) = 17.93$). For learning, a significant impairment occurs between w^{1118} and *dfmr1* ($p = 4.662 \times 10^{-7}$), and a significant improvement between *dfmr1* alone and with *UH1*-Gal4 driven UAS-*Trhn* ($p = 3.367 \times 10^{-9}$). No significant differences occur in any other comparisons. Memory performance also shows a significant effect of genotype ($F(4,75) = 10.58$). For memory trials, a significant impairment occurs between w^{1118} and *dfmr1* ($p = 3.902 \times 10^{-6}$), and significant improvement between *dfmr1* alone and with *UH1*-Gal4 driven UAS-*Trhn* ($p = 2.645 \times 10^{-6}$). No significant differences occur in any other comparisons. (**C**) Representative Mushroom Body lobe (anti-Trio, green outline) anti-serotonin (5-HT, grey scale) labeling in the same five above genotypes in untrained (top row) and trained (bottom row) conditions. Quantification of MB 5-HT fluorescence intensity from untrained (**D**) and T-maze trained (**E**) conditions. Data show individual brains (n = 10–15/condition), mean ± SEM, and one-way ANOVA with Tukey's multiple comparisons tests. For the untrained basal condition, the overall effect of genotype is significant ($F(4, 47) = 28.50$), with a significant elevation occurring between *dfmr1* nulls alone versus with *UH1*-Gal4 driven UAS-*Trhn* ($p = 1.477 \times 10^{-8}$). No significant differences occur in any other comparisons. For the T-maze trained condition, the overall effect of genotype is also significant ($F(4, 45) = 25.75$), with a significant increase between *dfmr1* nulls alone versus with *UH1*-Gal4 driven UAS-*Trhn* ($p = 2.207 \times 10^{-7}$). No significant differences occur in any other comparisons. Significance is indicated as $p > 0.05$ (not significant; ns) and $p < 0.0001$ (****).

Our previous studies demonstrate anti-5HT$_{2A}$R antibody specificity with cell-targeted *5HT$_{2A}$R* knockdown and overexpression[30]. Brains were washed 3 × for 20 min each with PBS-T and then incubated overnight with fluorescently-conjugated secondary antibodies. The secondary antibodies used were: AlexaFluor-488 goat anti-mouse (Invitrogen, A21202, 1:250) and AlexaFluor-555 donkey anti-rabbit (Invitrogen, A31572, 1:250). Brains were washed in PBS-T 3 × for 20 min each, followed by PBS and dH$_2$O 1 × for 20 min each. Brains were mounted in Fluoromount-G (EMS 17984-25) onto glass slides (75 × 25 mm, 0.9 to 1.06 mm; Corning) with a glass coverslip (No. 1.5H, Carl Zeiss). Double-sided adhesive tape (Scotch) was used to raise coverslips over the brains, with clear nail polish (Sally Hansen) used to seal the coverslip edges. All images were collected on a 510 META laser-scanning confocal microscope (Carl Zeiss) using either 40 × or 63 × oil-immersion objectives. All images were collected at 1024 × 1024 resolution with a Z-slice thickness of 0.75 µm. All confocal microscope imaging settings were kept absolutely constant in every experiment. All fluorescent measurement intensities were linear within the confocal range assayed. All the imaging quantifications were conducted blind to genotype and conditions, with the imaging analyses performed using the ImageJ Blind Analysis Tool.

Image quantification

Confocal image measurements were performed on Mushroom Body lobes as previously described[5]. Briefly,The MB lobes were labeled with anti-Trio (DSHB 9.4A) immunocytochemistry and then the MB was manually outlined to delineate the region of interest (ROI). Fluorescence intensity quantification was conducted within the outlined MB ROI for either anti-5-HT or 5-HT$_{2A}$R labeling as indicated, with the mean pixel fluorescence intensity values measured using NIH ImageJ as previously described[30,34]. All quantification measurements were done blind to both the genotype and training conditions using the ImageJ Blind Analysis Tool plug-in. All image acquisition settings, including the laser pinhole, gain, and offset, were held constant within every experiment. All raw images are available in the Harvard Dataverse under the "Kendal Broadie Dataverse" heading.

Statistical analyses

All comparisons were performed using Prism software (GraphPad version 9). For the different experiments, one-way analysis of variance (ANOVA) (Figs. 1, 2, 3, 5, and 6) or two-way ANOVA (Fig. 4) were used to assess changes among genotypes or treatment groups, followed by Tukey's multiple comparisons tests for multiple group comparisons. Sample sizes are specified in the figure legends. For behavioral assays, each data point represents one trial consisting of ~ 100 animals. For imaging assays, each data point represents one Mushroom Body lobe in a different brain. All the data meet normality and homogeneity of variance ANOVA requirements. Normality tests were conducted for every comparison. All datasets passed these criteria by using D' Agostino & Pearson tests. Data are presented as mean ± standard error of the mean (SEM). All mean ± SEM numerical values for both behavioral and imaging datasets are provided in Supplementary Table 1, with exact *p*-values reported. Significance in figures is indicated as $p < 0.05$ (*), $p < 0.01$ (**), $p < 0.001$ (***), and $p < 0.0001$ (****). Values of $p > 0.05$ are reported as not significant (ns). The exact *p*-values for all significant comparisons are also provided in the figure legends.

Results

The *Drosophila* FXS model and *5HT$_{2A}$R* knockdown share learning/memory deficits

Drosophila olfactory conditioning has been used for decades to dissect the genetic mechanisms of learning and memory[8,44]. Classical aversive conditioning is done in a T-maze with a conditioned stimulus (CS^+) odor paired to electric shock training versus an unconditioned stimulus (CS^-) odor, and then tests for the ability to discriminate between them (Fig. 1A). Testing can be done either immediately ("learning") or after a delay ("memory") to

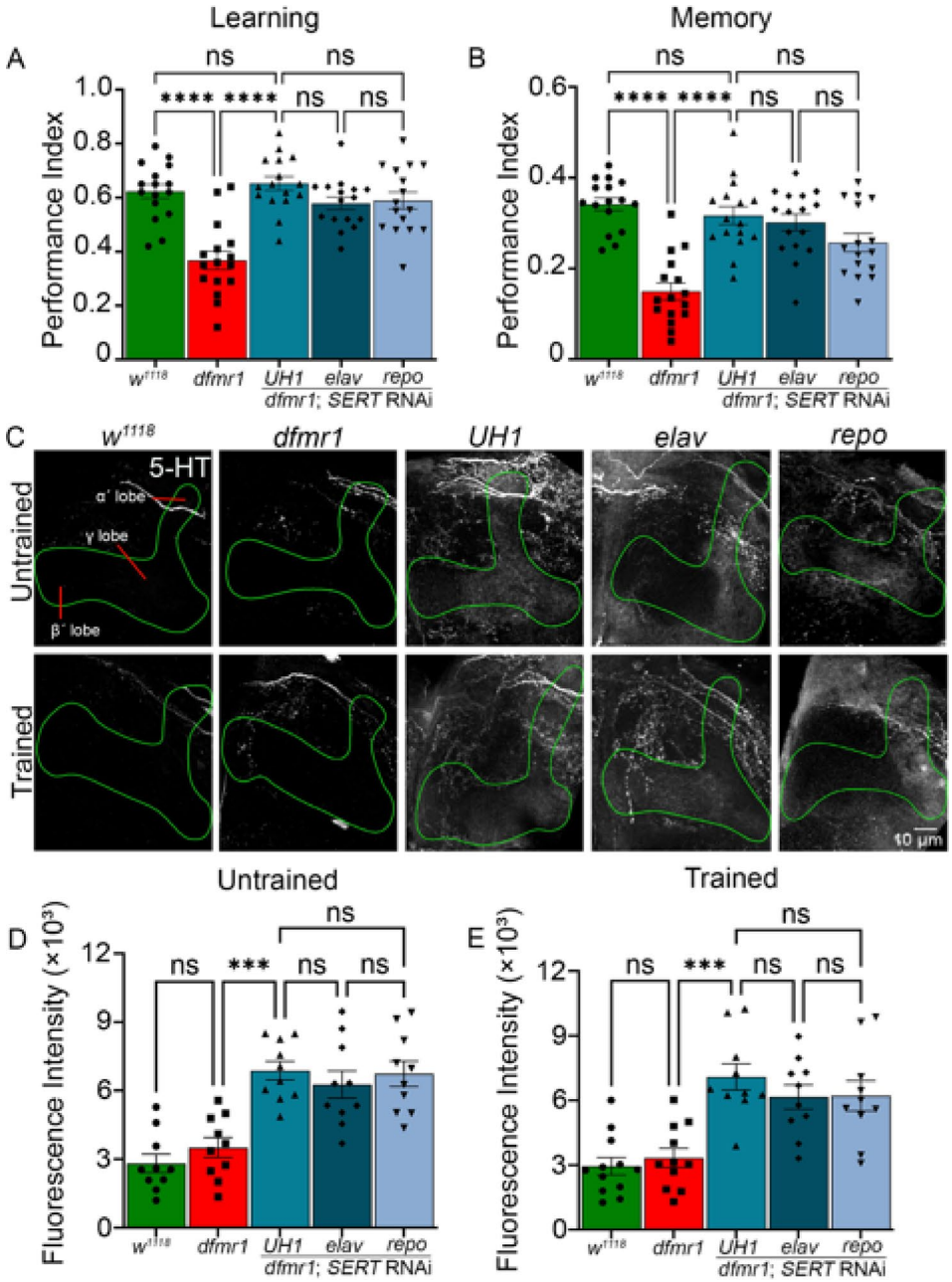

separate these two different behavioral phases (Fig. 1B). Performance index (PI) outcomes are quantified as $(CS^- - CS^+)/(CS^- + CS^+)$ for both learning and memory (Fig. 1C). To begin to test links between serotonin signaling and the FXS disease model (*dfmr1* null mutants), 5 genotypes were tested: the genetic background control (w^{1118}), a serotonin transporter knockdown (*SERT* RNAi), a serotonin receptor 2A knockdown ($5HT_{2A}R$ RNAi), *dfmr1* null mutants ($dfmr1^{\Delta 50M}$), and transgenic *UH1*-Gal4/ + driver in this background (*dfmr1* control). Compared to genetic background controls, *UH1*-Gal4 driven *SERT* RNAi has no significant effect on either the immediate learning or maintained memory outcomes (Fig. 1C), suggesting that elevated serotonin (5-HT) levels do not impact baseline behavioral performance. In contrast, $5HT_{2A}R$ RNAi significantly impairs both immediate learning ($p = 2.588 \times 10^{-4}$) and memory maintenance ($p = 6.347 \times 10^{-3}$), showing that reduced $5HT_{2A}R$ signaling causes learning and memory deficits (Fig. 1C). Similarly, the *dfmr1* null mutants have both significantly reduced learning ($p = 1.924 \times 10^{-6}$) and memory ($p = 3.0 \times 10^{-11}$), which are unaltered with the transgenic Gal4 driver control (Fig. 1C). These findings indicate $5HT_{2A}R$ and *dfmr1* loss similarly impair immediate learning, and both cause strong memory deficits, suggesting a possible role of serotonergic signaling in *Drosophila* FXS disease model behavioral phenotypes.

The *Drosophila* central brain Mushroom Body (MB) is the site of learning/memory circuitry (Fig. 1D, left)[45]. The MB circuit is composed of approximately 2,000 intrinsic MB neurons/hemisphere called Kenyon cells (KCs)[46], which extend their axons into discrete MB lobes (α/β, α′/β′, and γ; Fig. 1D, right) to form compartmentalized circuits that mediate associative learning and memory consolidation[47]. The KC γ neurons primarily mediate odorant associative learning[48], the α/β neurons contribute to memory retrieval[49,50], and the α′/β′neurons are essential for long-term memory (LTM) storage[50]. To study the MB circuit underlying the behavioral outcomes,

◀**Fig. 3**. Serotonin transporter (SERT) knockdown restores FXS learning/memory. Learning (**A**) and memory (**B**) performance index quantifications across five genotypes; genetic background control (w^{1118}; green), FXS model (*dfmr1*; red), and UAS-*serotonin transporter* (*SERT*) RNAi in the *dfmr1* mutant background driven by *UH1*- (ubiquitous), *elav*- (neuronal), and *repo*- (glial) Gal4 lines (blue). Data show individual trials (n = 16 each), mean ± SEM, and one-way ANOVA with Tukey's multiple comparisons tests. Learning performance shows a significant effect of genotype ($F(4,75) = 16.40$). For learning, a significant impairment occurs between w^{1118} and *dfmr1* ($p = 8.993 \times 10^{-6}$), and a significant improvement between *dfmr1* alone vs with *UH1*-Gal4 driven *SERT* RNAi ($p = 4.388 \times 10^{-7}$). No significant differences occur in any of the other comparisons. Memory performance also shows a significant effect of genotype ($F(4,75) = 17.00$). For memory, a significant impairment occurs between w^{1118} and *dfmr1* ($p = 6.184 \times 10^{-9}$), and significant improvement between *dfmr1* alone and with *UH1*-Gal4 driven UAS-*SERT* RNAi ($p = 6.644 \times 10^{-7}$). No significant differences occur in any other comparisons. (**C**) Mushroom Body lobe outline (anti-Trio, green) and anti-serotonin (5-HT, grey scale) labeling in the same five genotypes in untrained (top row) and trained (bottom row) conditions. Quantification of the MB 5-HT fluorescence intensity in both the untrained (**D**) and trained (**E**) conditions. Data show individual brains (n = 10–15/condition), mean ± SEM, and one-way ANOVA with Tukey's multiple comparisons tests. For the untrained condition, the overall effect of genotype is significant ($F(4, 45) = 15.62$), with a significant elevation occurs between *dfmr1* alone and with *UH1*-Gal4 driven UAS-*SERT* RNAi ($p = 1.285 \times 10^{-4}$). No significant differences occur in any of the other comparisons. For the trained condition, the overall effect of genotype is also significant ($F(4, 48) = 12.19$), with a significant increase likewise occurring between *dfmr1* alone and with *UH1*-Gal4 driven UAS-*SERT* RNAi ($p = 1.267 \times 10^{-4}$). No significant differences occur in any other comparisons. Significance is indicated as $p > 0.05$ (not significant; ns), $p < 0.001$ (***), and $p < 0.0001$ (****).

staged brains were visualized with anti-Trio labeling[5,51], which reveals the MB lobes in the context of the whole brain (Fig. 1D). High magnification imaging shows the α′, β′, and γ lobes that are the focus of our serotonin pathway studies (Fig. 1D, right). The recently released FlyWire codex allows complete 3D reconstruction to investigate MB serotonergic circuitry[52]. The serotonergic dorsal paired medial neuron (DPM, green) provides the principal MB serotonergic input (Fig. 1E. DPMs directly innervate MB Kenyon cells (magenta; only a small subset of KCs shown for clarity, providing widespread serotonergic modulation driving learning acquisition and memory consolidation[27,53]. The FlyWire connectome confirms extensive DPM processes overlapping the MB intrinsic circuitry, with defined synaptic inputs onto MB Kenyon cells, illuminating the spatial organization of serotonergic innervation in relation to this well-defined learning and memory circuit (Fig. 1E). Based on this behavioral and brain MB circuitry framework, we set forth to test the role of serotonergic signaling in *Drosophila* FXS model learning and memory impairments.

Tryptophan hydroxylase overexpression restores FXS model learning and memory

The rate-limiting serotonin biosynthetic enzyme is tryptophan hydroxylase (Trhn)[54]. *Trhn* overexpression elevates 5-HT levels and potentiates serotonergic signaling[30,55]. To investigate whether increasing serotonin could modulate learning/memory impairments in the *Drosophila* FXS disease model (*dfmr1* null mutants), we overexpressed UAS-*Trhn*[41] using three drivers: ubiquitious (*UH1*-Gal4), neuronal (*elav*-Gal4), and glial (*repo*-Gal4). qPCR testing *Trhn* overexpression (OE) demonstrates this transgenic method is highly efficacious (*UH1*-Gal4/w^{1118} vs. *UH1*-Gal4; UAS-*Trhn* $\Delta\Delta C_q$ 14.31 ± 0.108, $p = 1.962 \times 10^{-7}$). All *Trhn* overexpression genotypes were tested alongside Gal4 driver (*UH1*-Gal4/w^{1118}, *elav*-Gal4/w^{1118}, *repo*-Gal4/w^{1118}) as well as the UAS transgene (UAS-*Trhn*/w^{1118}) controls. Compared to the genetic background control (w^{1118}), *dfmr1* null mutants have a significant learning impairment ($p = 4.662 \times 10^{-7}$), which can be restored by *UH1*-Gal4 driven *Trhn* overexpression, significantly improving learning relative to the *dfmr1* nulls ($p = 3.367 \times 10^{-9}$) and resulting in a performance that shows no significant difference from w^{1118} controls ($p = 0.7789$; Fig. 2A). Consistently, neuronal *elav*-Gal4 driven *Trhn* overexpression results in a comparable improvement in FXS model learning, and we were surprised that glial overexpression also proved efficacious (Fig. 2A, right). For memory compared to controls, ubiquitous *Trhn* overexpression in *dfmr1* mutants restores performance ($p = 3.902 \times 10^{-6}$) and improves memory over *dfmr1* nulls ($p = 2.645 \times 10^{-6}$), with no significant difference left to genetic background controls ($p = 0.9999$; Fig. 2B). As above, neuronal (*elav*-Gal4) and glial (*repo*-Gal4) *Trhn* overexpression in *dfmr1* mutants similarly corrects memory, with no significant differences among the three drivers, albeit with a trend towards an additive effect from neuronal *elav*-Gal4 and glial *repo*-Gal4 compared to the ubiquitous *UH1*-Gal4 (Fig. 2B, right). The 3 Gal4 driver and UAS-Trhn controls showed no behavior differences compared to the w^{1118} genetic background. These findings suggest elevated serotonin signaling is sufficient to restore learning/memory in the *Drosophila* FXS model.

To assay serotonin signaling in the underlying Mushroom Body (MB) circuitry, all genotypes were labeled with anti-5-HT[30], both under baseline, untrained conditions and following the above training protocol (Fig. 2C). Serotonin levels were imaged by delineating the MB with anti-Trio labeling[5]. Anti-Trio images used to delineate the MB lobes (green outlines, Fig. 2C) are shown for all genotypes and conditions (Fig. S1). The genetic background control (w^{1118}) and FXS disease model (*dfmr1* null mutants) exhibit low basal levels of serotonin, with *Trhn* overexpression dramatically elevating serotonin (Fig. 2C, top row). T-maze aversive olfactory conditioning training does not detectably alter serotonin in any of the genotypes (Fig. 2C, bottom row). Anti-Trio immunostaining was performed in all trials, but was not displayed for clarity; the anti-trio outline was used to define the MB quantification region. The anti-5-HT fluorescence intensity was quantified within the MB (sum of slices) to quantitatively compare serotonin levels. In untrained conditions, there is no significant

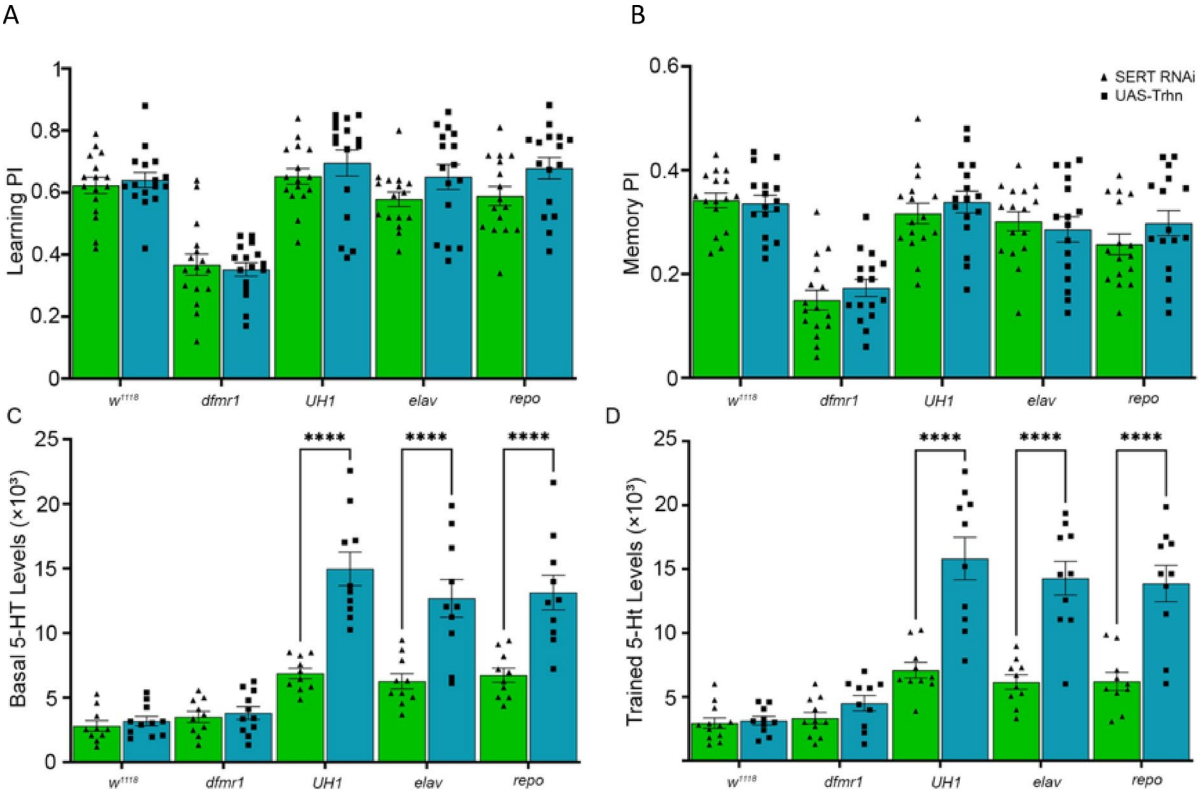

Fig. 4. Comparison of the *Trhn* overexpression and *SERT* knockdown effects. Quantification of performance index in learning (**A**) and memory (**B**) assays by genotype, tested with either *Trhn* overexpression (OE, blue) or *SERT* knockdown (RNAi, green). Genotypes include genetic background control (w^{1118}), FXS model (*dfmr1*), and both UAS transgenes in the *dfmr1* null background driven by *UH1*- (ubiquitous), *elav*- (neuronal), and *repo*- (glial) Gal4 lines. Data show individual trials (n = 16 per condition), mean ± SEM, and one-way ANOVA with Tukey's multiple comparisons tests. For learning, the two-way ANOVA reveals no significant interaction between genotype and training ($F(4,150) = 0.9138$), a significant effect of genotype ($F(4,150) = 33.16$), and no significant effect of *Trhn* overexpression versus *SERT* knockdown ($F(1,150) = 4.454$). Similarly, for memory, the two-way ANOVA reveals no significant interaction between genotype and training ($F(4,150) = 0.7009$), a significant effect of genotype ($F(4,150) = 26.12$), and no significant effect of Trhn overexpression versus SERT knockdown ($F(1,150) = 1.093$). Quantification of basal (**C**) and trained (**D**) 5-HT fluorescence intensities in the Mushroom Body across the same genotypes and conditions. Data points show results from individual brains (n = 10–15 per condition), mean ± SEM, and one-way ANOVA with Tukey's multiple comparisons tests. For the basal condition, the two-way ANOVA shows no significant interaction between genotype and training ($F(4,92) = 9.901$), a significant main effect of genotype ($F(4,92) = 40.85$), and no significant main effect of *Trhn* overexpression versus *SERT* RNAi ($F(1,92) = 66.85$). In the basal condition, significant differences in 5-HT intensity occur between *Trhn* OE and *SERT* RNAi with *UH1*- ($p = 4.785 \times 10^{-8}$), *elav*- ($p = 2.325 \times 10^{-5}$), and *repo*- ($p = 2.528 \times 10^{-5}$) Gal4 drivers. For the trained condition, the two-way ANOVA likewise shows no significant interaction ($F(4,93) = 10.64$), significant effect of genotype ($F(4,93) = 38.50$), and no significant effect of training ($F(1,93) = 81.86$). In the trained condition, significant differences also occur between *Trhn* OE and *SERT* RNAi with *UH1*- ($p = 5.731 \times 10^{-8}$), *elav*- ($p = 4.934 \times 10^{-7}$), and *repo*- ($p = 2.470 \times 10^{-6}$) drivers. Significance is indicated as $p < 0.0001$ (****).

difference between control and *dfmr1* nulls ($p = 0.9927$), indicating that basal serotonin levels are not detectably affected by *dfmr1* loss alone (Fig. 2D, left). Compared to the *dfmr1* mutants, the *Trhn* overexpression results in a highly significant elevation of serotonin in the MB (*UH1*-Gal4 driven *Trhn* overexpression; $p = 1.477 \times 10^{-8}$), with a similar elevation from the other drivers (Fig. 2D, right). In the trained condition, results are similar, with no significant difference between w^{1118} and *dfmr1* nulls ($p = 0.9231$), compared to a highly significant serotonin elevation arising from *UH1*-Gal4 driven *Trhn* overexpression ($p = 2.207 \times 10^{-7}$; Fig. 2E). There is a trend towards an additive effect from *elav*- and *repo*-Gal4 versus ubiquitous *UH1*-Gal4, but no significant differences (Fig. 2D,E). All 3 Gal4 (*UH1*-Gal4/w^{1118}, *elav*-Gal4/w^{1118}, *repo*-Gal4/w^{1118}) and UAS transgene (UAS-*Trhn*/w^{1118}) controls display 5-HT levels indistinguishable from the w^{1118} background control (Fig. S2). Taken together, these findings suggest elevating brain serotonin levels restores learning and memory to control levels within detectable limits in the *Drosophila* FXS disease model.

Serotonin transporter knockdown likewise corrects FXS model learning/memory

To independently test whether increasing serotonin signaling can correct learning and memory deficits in the *dfmr1* null mutants—and to distinguish whether serotonin synthesis or reuptake contributes differentially to this restorative effect—we next tested whether inhibiting the serotonin transporter (SERT) could replicate the behavioral and molecular changes compared to *Trhn* overexpression. SERT inhibition prevents serotonin reuptake to elevate serotonin levels in the brain[56]. We employed a UAS-*SERT* RNAi[42] in the *dfmr1* null mutants using the same three Gal4 drivers above to transgenically control serotonin reuptake in our FXS disease model. All *SERT* RNAi genotypes were tested beside both Gal4 drivers alone (*UH1*-Gal4/w^{1118}, *elav*-Gal4/w^{1118}, *repo*-Gal4/w^{1118}) and UAS-transgene (*SERT* RNAi/w^{1118}) controls, which all performed at w^{1118} levels (Fig. 1C). Compared to the genetic background control (w^{1118}), the *dfmr1* null mutants again exhibit significant learning ($p = 8.993 \times 10^{-6}$) and memory ($p = 6.184 \times 10^{-9}$) impairments (Fig. 3A,B). Ubiquitous *SERT* knockdown in the *dfmr1* null mutants (*UH1*-Gal4 driven UAS-*SERT* RNAi) significantly improves learning performance compared to the *dfmr1* null mutants ($p = 4.388 \times 10^{-7}$), restoring behavior that is statistically indistinguishable from the genetic controls ($p = 0.9998$; Fig. 3A, middle). Likewise, global *UH1*-driven *SERT* RNAi significantly improves memory performance compared to the *dfmr1* null mutants ($p = 6.644 \times 10^{-7}$), correcting memory performance back to control levels, with no statistical difference remaining compared to the w^{1118} genetic background animals ($p = 0.9960$; Fig. 3B, middle). Neuronal (*elav*-Gal4) and glial (*repo*-Gal4) *SERT* knockdown show similar restoration of learning and memory, with no significant differences between any of the three different Gal4 driver lines (Fig. 3A,B). These findings suggest that serotonin transporter inhibition (*SERT* RNAi) is sufficient to restore both learning and memory performance in the *Drosophila* FXS disease model.

To test whether *SERT* knockdown increases brain serotonin levels as expected, we performed anti-5-HT labeling in the basal untrained and T-maze trained conditions in all the genotypes (Fig. 3C). All of the control genotypes (*UH1*-Gal4/w^{1118}, *elav*-Gal4/w^{1118}, *repo*-Gal4/w^{1118}, and UAS-*SERT* RNAi/ w^{1118}) display 5-HT levels comparable to w^{1118}, indicating that any observed changes are specific to *SERT* knockdown (Fig. S2). With MB anti-Trio labeling, serotonin levels are again very low in genetic background control (w^{1118}) and FXS model (*dfmr1* nulls) in both treatment conditions (Fig. 3C). *SERT* RNAi increases serotonin levels within the MB, but to a much lower extent than the previous *Trhn* overexpression effects (compare Figs. 2C and 3C). T-maze aversive conditioning training does not detectably alter serotonin compared to baseline in any of the genotypes (Fig. 3C, bottom row). Anti-Trio immunostaining was performed in all trials, with the outline displayed used for quantification. In the anti-Trio defined MB, the anti-5-HT fluorescence intensity was quantified across untrained and trained conditions. In the basal state, there is again no significant differences between w^{1118} controls and *dfmr1* mutants ($p = 0.8508$), but serotonin levels are significantly elevated by ubiquitous *SERT* knockdown in *dfmr1* mutants (*UH1*-Gal4 *SERT* RNAi) compared to *dfmr1* alone ($p = 1.285 \times 10^{-4}$; Fig. 3D). There are no significant differences between the three *SERT* knockdown conditions, suggesting that the serotonin transporter operates in both neurons and glia to limit 5-HT levels in the MB. With T-maze training, there is still no significant difference in MB serotonin levels in the w^{1118} controls and *dfmr1* mutants ($p = 0.9839$), but *UH1*-driven *SERT* RNAi again significantly increases 5-HT levels compared to the *dfmr1* nulls ($p = 1.267 \times 10^{-4}$; Fig. 3E). There is a trend for additive effect from *elav*-Gal4 and *repo*-Gal4 towards *UH1*-Gal4, but no significant differences. Taken together, these findings suggest elevating serotonin by two independent methods restores learning/memory in the *Drosophila* FXS model.

Elevating serotonin levels via *Trhn* overexpression (increasing 5-HT synthesis) or *SERT* knockdown (reducing 5-HT reuptake) appears to produce comparable restoration of FXS model learning and memory. To weigh the relative efficacy of these two strategies, we directly compare the UAS-*Trhn* overexpression (blue) and UAS-*SERT* RNAi (green) effects on *dfmr1* mutants (Fig. 4). Quantification of the learning performance index (PI) reveals that both approaches produce comparable results, with no significant differences between the genetic background controls (w^{1118}), FXS model (*dfmr1*), or the transgenes driven with any of the three Gal4 drivers (Fig. 4A). Likewise, memory performance was indistinguishable in both manipulations, with no significant differences between the five genotypes with either *Trhn* overexpression or *SERT* knockdown (Fig. 4B). These findings suggest that both transgenic strategies effectively restore learning and memory in *dfmr1* null mutants, and that neither method yields more benefit. However, 5-HT analyses reveal significant differences in MB serotonin elevation with the two approaches. In the basal, untrained condition, *Trhn* overexpression promotes significantly greater serotonin levels compared to *SERT* RNAi under *UH1*- ($p = 4.785 \times 10^{-8}$), *elav*- ($p = 2.325 \times 10^{-5}$), and *repo*- ($p = 2.528 \times 10^{-5}$) Gal4 driver expression (Fig. 4C). For the T-maze trained condition, *Trhn* overexpression continues to elevate serotonin more than the *SERT* RNAi counterparts between *UH1*- ($p = 5.731 \times 10^{-8}$), *elav*- ($p = 4.934 \times 10^{-7}$), and *repo*- ($p = 2.470 \times 10^{-6}$) drivers (Fig. 4D). These findings show *Trhn* overexpression and *SERT* knockdown both restore behavioral performance, but with distinct magnitudes of serotonin elevation. We next turned to testing the role of serotonin receptors within our FXS disease model.

Serotonin receptor 2A knockdown phenocopies FXS model learning and memory

The behavioral correction of *dfmr1* mutants with *Trhn* overexpression or *SERT* knockdown suggests increasing serotonin signaling can ameliorate learning and memory deficits in this FXS model. However, the serotonin receptor involved in this mechanism needed to be tested. One candidate is serotonin receptor 2A ($5HT_{2A}R$)[57], which is strongly implicated in learning/memory function[21]. To test $5HT_{2A}R$ requirements, we used a UAS-$5HT_{2A}R$ RNAi[34,43] driven in the *dfmr1* null mutant using the same three Gal4 drivers employed above. All 5-$HT_{2A}R$ RNAi genotypes were tested alongside Gal4 drivers alone (*UH1*-Gal4/w^{1118}, *elav*-Gal4/w^{1118}, *repo*-Gal4/w^{1118}) as well as the UAS transgene alone (UAS-5-$HT_{2A}R$ RNAi/ w^{1118}), which all performed at the w^{1118} level (Fig. 1C; Fig. S3). Compared to w^{1118} background control, *dfmr1* nulls again have significantly lower learning ($p = 7.460 \times 10^{-5}$) and memory ($p = 8.599 \times 10^{-5}$) behavior performance (Fig. 5A,B). In learning, ubiquitous $5HT_{2A}R$ knockdown with *UH1*-Gal4 only slightly, albeit significantly, increases the *dfmr1* null

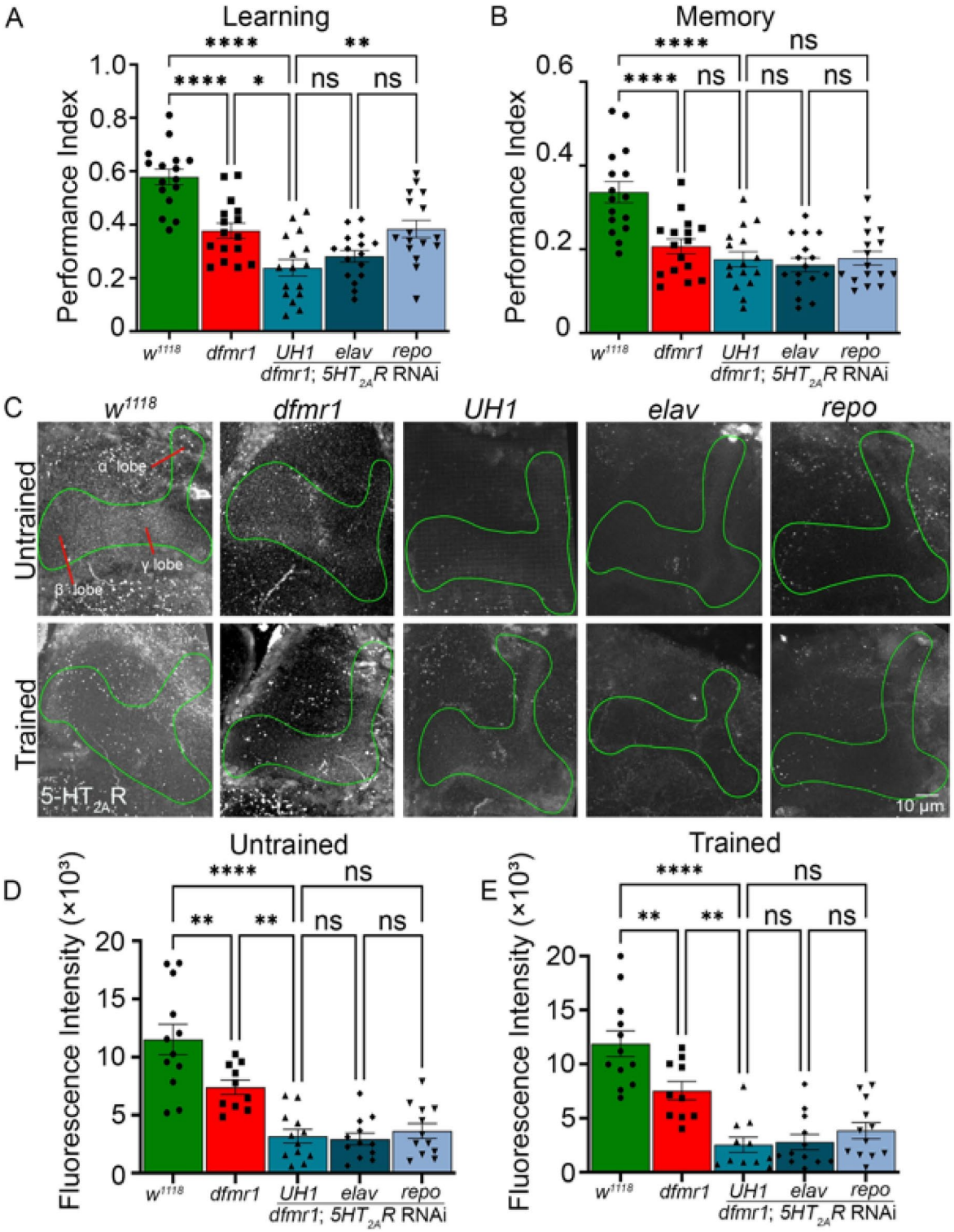

mutant impairment ($p = 0.01548$) which, together with the strong $5HT_{2A}R$ RNAi impact alone in the control background ($p = 2.588 \times 10^{-4}$; Fig. 1C), suggests a large contribution of $5HT_{2A}R$ loss to the FXS model deficit (Fig. 5A). Global *UH1*-Gal4 driven $5HT_{2A}R$ RNAi in *dfmr1* nulls remains significantly impaired relative to w^{1118} ($p = 4.6 \times 10^{-10}$), suggesting a critical requirement in immediate learning. The neuronal *elav*-Gal4 outcome is not significantly different from *UH1*-Gal4 ($p = 0.9093$), but glial *repo*-Gal4 is significantly different ($p = 9.559 \times 10^{-3}$), showing the $5HT_{2A}R$ requirement is solely in neurons (Fig. 5A). For memory, ubiquitous $5HT_{2A}R$ RNAi causes no difference from *dfmr1* null mutants alone ($p = 0.8586$), remaining significantly impaired versus w^{1118} controls ($p = 7.094 \times 10^{-7}$; Fig. 5B). There are no significant differences between or within the three Gal4 drivers. These findings suggest neuronal $5HT_{2A}R$ enables learning in concert with *dfmr1* function.

To test $5HT_{2A}R$ expression in the MB learning circuit, dual anti-$5HT_{2A}R$ and -Trio co-labeling was done in both untrained and T-maze trained conditions (Fig. 5C). Genetic background controls (w^{1118}) exhibit high

◀**Fig. 5**. *5HT$_{2A}$R* knockdown only weakly exacerbates FXS model learning/memory. Performance index quantifications of learning (**A**) and memory (**B**) across five genotypes; the genetic background control (w^{1118}; green), FXS model (*dfmr1*; red), and UAS-*5HT$_{2A}$ receptor* (*5HT$_{2A}$R*) RNAi in the *dfmr1* null background driven by *UH1*- (ubiquitous), *elav*- (neuronal), and *repo*- (glial) Gal4 lines (blue). Data show all individual trials (n = 16 each), mean ± SEM, and one-way ANOVA with Tukey's multiple comparisons tests. Learning performance shows a significant effect of genotype ($F(4,75) = 21.02$). For learning, significant differences occur between w^{1118} and *dfmr1* ($p = 7.460 \times 10^{-5}$), w^{1118} and *UH1*-Gal4 driven *5HT$_{2A}$R* RNAi in the *dfmr1* null mutant ($p = 4.617 \times 10^{-10}$), and between this condition and *repo*-Gal4 driven *5HT$_{2A}$R* RNAi in the *dfmr1* mutant ($p = 9.559 \times 10^{-3}$). A significant difference also occurs between *dfmr1* and *UH1*-Gal4 driven *5HT$_{2A}$R* RNAi in the *dfmr1* mutant ($p = 0.01548$). No significant differences occur in the other comparisons. Memory performance also shows a significant effect of genotype ($F(4,75) = 14.04$). For memory, significant differences occur between w^{1118} and *dfmr1* ($p = 8.599 \times 10^{-5}$), and between w^{1118} and *UH1*-Gal4 driven *5HT$_{2A}$R* RNAi in the *dfmr1* mutant ($p = 7.094 \times 10^{-7}$). No other significant differences occur. (**C**) Representative Mushroom Body lobe (anti-Trio, green outline) anti-serotonin receptor 2A (5HT$_{2A}$R, grey scale) labeling in the same five genotypes in untrained (top row) and trained (bottom row) conditions. Quantification of MB 5-HT fluorescence intensity from untrained (**D**) and trained (**E**) conditions. Data show individual brains (n = 10–15 per condition), mean ± SEM, and one-way ANOVA with Tukey's multiple comparisons tests. For the basal untrained condition, the overall effect of genotype is significant ($F(4, 53) = 21.92$), with a significant difference occurs between w^{1118} and *dfmr1* ($p = 7.858 \times 10^{-3}$), w^{1118} and *UH1*-Gal4 driven *5HT$_{2A}$R* RNAi in the *dfmr1* mutant ($p = 7.621 \times 10^{-9}$), and *dfmr1* and *UH1*-Gal4 driven *5HT$_{2A}$R* RNAi in the *dfmr1* mutant ($p = 5.732 \times 10^{-3}$). No significant differences occur in the other comparisons. For the trained condition, the overall effect of genotype is significant ($F(4, 52) = 21.58$), with a significant 5HT$_{2A}$R loss occurring between w^{1118} and *dfmr1* null ($p = 9.630 \times 10^{-3}$), w^{1118} and *UH1*-Gal4 driven *5HT$_{2A}$R* RNAi in the *dfmr1* null mutant ($p = 5.083 \times 10^{-9}$), and *dfmr1* and *UH1*-Gal4 driven *5HT$_{2A}$R* RNAi in the *dfmr1* null mutant ($p = 2.454 \times 10^{-3}$). No other significant differences occur. Significance is indicated as $p > 0.05$ (not significant, ns), $p < 0.05$ (*), $p < 0.01$ (**), and $p < 0.0001$ (****).

5HT$_{2A}$R puncta within and around the MB lobes compared to strongly reduced 5HT$_{2A}$R puncta in the FXS disease model (Fig. 5C, left). Knockdown of *5HT$_{2A}$R* with all Gal4 drivers nearly abolishes detectable 5HT$_{2A}$R labeling, suggesting interconnected 5HT$_{2A}$R maintenance in the neurons and glia (Fig. 5C, right). T-maze aversive conditioning training does not detectably alter MB 5HT$_{2A}$R levels in any of the five genotypes (Fig. 5C, bottom row). Quantification of anti-5HT$_{2A}$R fluorescence intensity within the MB lobes reveals a significant decrease in the *dfmr1* null mutants compared to the w^{1118} background controls ($p = 7.858 \times 10^{-3}$; Fig. 5D), suggesting the FXS model has lower 5HT$_{2A}$R levels in the learning circuit. Control genotypes (*UH1*-Gal4/w^{1118}, *elav*-Gal4/w^{1118}, *repo*-Gal4/w^{1118}, and UAS-*5-HT$_{2A}$R* RNAi/w^{1118}) show 5-HT$_{2A}$R levels comparable to w^{1118} alone, confirming a reduction specific to *dfmr1* loss. In the untrained condition, ubiquitous *5HT$_{2A}$R* knockdown in the *dfmr1* null mutants causes significantly reduced fluorescence intensity compared to both w^{1118} controls ($p = 7.621 \times 10^{-9}$) and *dfmr1* nulls ($p = 5.732 \times 10^{-3}$; Fig. 5D, right). No significant differences occur between the three Gal4 drivers. Following T-maze training, *dfmr1* mutants continue to exhibit reduced 5HT$_{2A}$R level compared to w^{1118} controls ($p = 9.630 \times 10^{-3}$), consistent with basal conditions (Fig. 5E). Likewise, 5HT$_{2A}$R levels remain significantly reduced with *UH1*-driven *5HT$_{2A}$R* RNAi in *dfmr1* nulls compared to *dfmr1* mutants alone ($p = 2.454 \times 10^{-3}$) and w^{1118} controls ($p = 5.083 \times 10^{-9}$; Fig. 5E). No significant differences are detected among the Gal4 drivers. These findings show a loss of 5HT$_{2A}$ receptors in *dfmr1* mutants, and suggest *5HT$_{2A}$R* overexpression should rectify *Drosophila* FXS disease model phenotypes.

5HT$_{2A}$R overexpression restores learning and memory in the FXS disease model

To test whether elevating serotonin receptor 2A (5HT$_{2A}$R) signaling can restore learning and memory in *dfmr1* nulls, we overexpressed UAS-*5HT$_{2A}$R*[43]. Our hypothesis is that 5HT$_{2A}$R loss in the FXS disease model results in impaired learning and memory, which should be corrected by potentiating 5-HT signaling either by elevating 5-HT levels (Figs. 2, 3, and 4) or increasing 5HT$_{2A}$R expression. All 5-HT$_{2A}$R overexpression genotypes were tested alongside Gal4 driver alone (*UH1*-Gal4/w^{1118}, *elav*-Gal4/w^{1118}, *repo*-Gal4/w^{1118}) and UAS-transgene (UAS-*5-HT$_{2A}$R*/ w^{1118}) controls, which all performed at w^{1118} levels. Compared to genetic background controls (w^{1118}), *dfmr1* nulls once again show a very significantly impaired learning ($p = 4.112 \times 10^{-7}$) and memory ($p = 2.133 \times 10^{-5}$) performance (Fig. 6A,B). For learning, ubiquitous UAS-*5HT$_{2A}$R* overexpression with the *UH1*-Gal4 driver in the *dfmr1* null significantly restores memory performance relative to *dfmr1* alone ($p = 2.404 \times 10^{-5}$), to a level not significantly different from the w^{1118} controls ($p = 0.8517$), indicating a complete behavioral correction (Fig. 6A). *UH1*-driven *5HT$_{2A}$R* overexpression results in significantly better performance than the *repo*-driven receptor ($p = 8.799 \times 10^{-3}$), suggesting a selective 5HT$_{2A}$R role in neurons. Consistently, there is no significant difference between *UH1*- and *elav*-Gal4 *5HT$_{2A}$R* overexpression ($p = 0.3961$), indicating neuronal 5HT$_{2A}$R function (Fig. 6A). For memory performance, the *UH1*-driven *5HT$_{2A}$R* overexpression significantly improves behavioral outcomes compared to *dfmr1* null mutant alone ($p = 2.762 \times 10^{-4}$), with the restored memory performance not significantly different from the w^{1118} controls ($p = 0.9604$), indicating a complete behavioral rectification (Fig. 6B). There is no significant difference between the three Gal4 drivers. Transgenic controls (*UH1*-Gal4/w^{1118}, *elav*-Gal4/w^{1118}, *repo*-Gal4/w^{1118}, and UAS-*5HT$_{2A}$R*/w^{1118}) show no significant behavioral differences from w^{1118}, confirming rescue is specific to *5-HT$_{2A}$R* overexpression (Fig. S3). These findings indicate *5-HT$_{2A}$R* overexpression can strongly restore both learning and memory performance in the *Drosophila* FXS disease model.

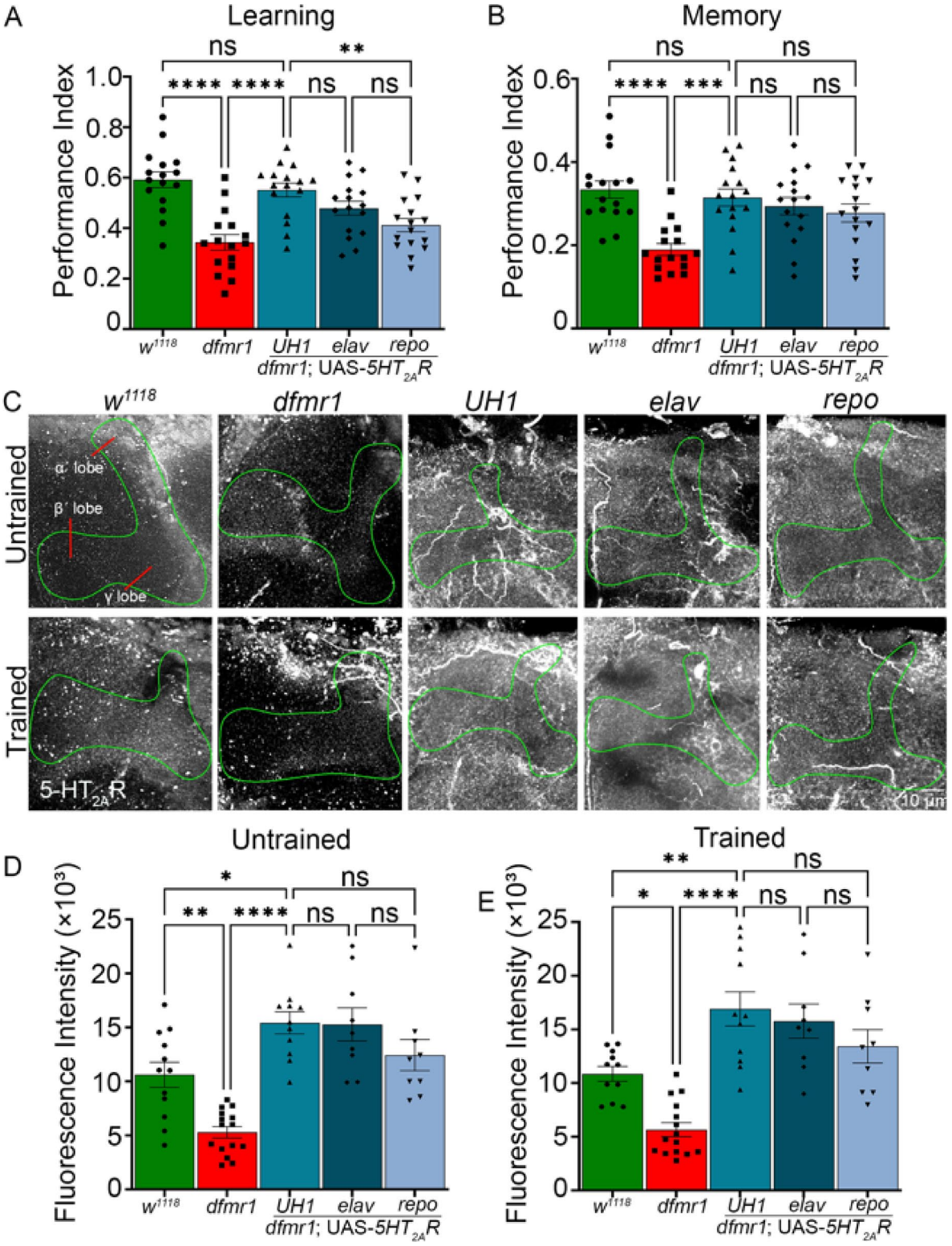

To test $5HT_{2A}R$ levels in the MB circuit, brains from all five genotypes were double labeled for anti-Trio and anti-$5HT_{2A}R$ in both untrained and trained conditions (Fig. 6C). For best image clarity, only the MB outline derived from anti-Trio is displayed. Genetic background controls (w^{1118}) show high $5HT_{2A}R$ puncta compared to many fewer $5HT_{2A}R$ puncta in the FXS disease model (Fig. 6C, left). *5HT$_{2A}$R* overexpression with all three Gal4 drivers increase the $5HT_{2A}R$ levels, again suggesting interconnected $5HT_{2A}R$ expression in MB neurons and glia (Fig. 6C, right). T-maze aversive conditioning training does not detectably alter $5HT_{2A}R$ levels in the MB circuit of any of the tested genotypes (Fig. 6C, bottom row). Quantification of anti-$5HT_{2A}R$ fluorescence intensity within the MB shows a very significant loss in *dfmr1* null mutants compared to the w^{1118} background controls ($p = 3.495 \times 10^{-3}$; Fig. 6D), again indicating the FXS disease model has reduced $5HT_{2A}R$ levels in the MB circuit. Control genotypes (*UH1*-Gal4/w^{1118}, *elav*-Gal4/w^{1118}, *repo*-Gal4/w^{1118}, and UAS-*5HT$_{2A}$R*/w^{1118}) display

◀**Fig. 6**. *5HT$_{2A}$R* overexpression rectifies FXS model learning/memory performance. Learning (**A**) and memory (**B**) performance index quantifications across five genotypes; genetic background control (w^{1118}; green), FXS model (*dfmr1*; red), and UAS-*5HT$_{2A}$ receptor* (*5HT$_{2A}$R*) overexpression in the *dfmr1* background driven by *UH1-* (ubiquitous), *elav-* (neuronal), and *repo-* (glial) Gal4 lines (blue). Data show individual trials (n = 16 each), mean ± SEM, and one-way ANOVA with Tukey's multiple comparisons tests. Learning performance shows a significant effect of genotype ($F(4,75) = 21.30$). For learning, a significant impairment occurs between w^{1118} and *dfmr1* ($p = 4.112 \times 10^{-7}$), improvement compared to *dfmr1* with *UH1*-Gal4 driven UAS-*5HT$_{2A}$R* in the *dfmr1* null ($p = 2.404 \times 10^{-5}$), and decrease from the *UH1-* to *repo*-Gal4 conditions ($p = 8.799 \times 10^{-3}$). Memory performance also shows a significant effect of genotype ($F(4,75) = 7.881$). For memory, a significant loss again occurs between w^{1118} and *dfmr1* ($p = 2.133 \times 10^{-5}$), which is restored comparing *dfmr1* to *UH1*-Gal4 driven UAS-*5HT$_{2A}$R* in the *dfmr1* null ($p = 2.762 \times 10^{-4}$). No significant differences occur in the other comparisons. (**C**) Mushroom Body lobe (anti-Trio, green outline) anti-serotonin receptor 2A (5HT$_{2A}$R, grey scale) labeling in the same five genotypes in the untrained (top row) and trained (bottom row) conditions. Quantification of the MB 5-HT$_{2A}$R fluorescence intensity in the untrained (**D**) and trained (**E**) conditions. Data show individual brains (n = 10–15 per condition), mean ± SEM, and one-way ANOVA with Tukey's multiple comparisons tests. For the untrained condition, the overall effect of genotype is significant ($F(4, 51) = 16.85$), with a significant decrease occurs between w^{1118} and *dfmr1* ($p = 3.495 \times 10^{-3}$), w^{1118} and *UH1*-Gal4 driven UAS-*5HT$_{2A}$R* in *dfmr1* ($p = 2.067 \times 10^{-2}$), and between *dfmr1* and *UH1*-Gal4 driven UAS-*5HT$_{2A}$R* in *dfmr1* ($p = 4.722 \times 10^{-8}$). For the trained condition, the overall effect of genotype is significant ($F(4, 50) = 16.48$), with a significant loss between w^{1118} and *dfmr1* ($p = 1.423 \times 10^{-2}$), w^{1118} and *UH1*-Gal4 driven UAS-*5HT$_{2A}$R* in *dfmr1* ($p = 6.309 \times 10^{-3}$), and between *dfmr1* and *UH1*-Gal4 driven UAS-*5HT$_{2A}$R* in the *dfmr1* null ($p = 3.127 \times 10^{-8}$). No significant differences occur in other comparisons. Significance is indicated as $p > 0.05$ (not significant, ns), $p < 0.05$ (*), $p < 0.01$ (**), $p < 0.001$ (***), and $p < 0.0001$ (****).

5-HT$_{2A}$R levels comparable to w^{1118}, indicating the observed increase is specific to 5-HT$_{2A}$R overexpression. In the basal, untrained condition, *UH1*-driven *5HT$_{2A}$R* overexpression in the *dfmr1* null mutants very significantly elevates MB 5HT$_{2A}$R levels compared to *dfmr1* alone ($p = 4.722 \times 10^{-8}$) and more weakly compared to the w^{1118} background controls ($p = 2.067 \times 10^{-2}$), confirming successful overexpression (Fig. 6D). There are no significant differences between the Gal4 drivers. Following T-maze training, the same pattern is present with significantly lower MB 5HT$_{2A}$R levels in *dfmr1* mutants compared to matched controls ($p = 1.423 \times 10^{-2}$) and a very significant increase with *5HT$_{2A}$R* overexpression in *dfmr1* null mutants, strongly compared to *dfmr1* alone ($p = 3.127 \times 10^{-8}$) and more weakly compared to w^{1118} controls ($p = 6.309 \times 10^{-3}$; Fig. 6E). Taken together, these findings indicate that loss of 5HT$_{2A}$R signaling causes learning and memory deficits in *dfmr1* mutants and that 5HT$_{2A}$R overexpression can correct these impairments in the *Drosophila* FXS disease model.

Discussion

Fragile X syndrome (FXS) results from epigenetic loss of the Fragile X Messenger Ribonucleoprotein (FMRP), an mRNA-binding protein tightly regulating the translation of proteins critical for synaptic plasticity[58,59]. Like FXS patients, mouse and *Drosophila* FXS models exhibit deficient learning/memory[60,61], behaviors known to be modulated by serotonin[20,62]. Using classical olfactory aversive conditioning[44], we find loss of FMRP and 5-HT$_{2A}$R similarly impairs learning and memory (Fig. 1). Elevating serotonin via overexpression of the biosynthetic enzyme Trhn (Fig. 2) or SERT transporter knockdown (Fig. 3) restores learning and memory performance to control levels within detectable limits in the *dfmr1* null mutants. These complementary approaches are equally efficacious in correcting both of the behavioral outcomes, although Trhn overexpression drives much higher serotonin levels in the Mushroom Body (MB) learning/memory circuit (Fig. 4). The *Drosophila* FXS model shows reduced 5-HT$_{2A}$R levels, and *5-HT$_{2A}$R* knockdown only weakly exacerbates the *dfmr1* null mutant learning impairment, without any worsening of the memory deficit (Fig. 5). Consistently, *5-HT$_{2A}$R* overexpression within our FXS model restores normal learning and memory in *dfmr1* null mutants (Fig. 6). Thus, the *Drosophila* FXS disease model has strongly impaired 5-HT$_{2A}$R signaling, and elevating either 5-HT or 5-HT$_{2A}$R levels effectively restores *Drosophila* FXS disease learning and memory performance. Note all conclusions are based on associative olfactory conditioning and focus specifically on the Mushroom Body circuit, and therefore may not reflect broader FXS processes.

Null *dfmr1* mutants exhibit significant deficits in classical olfactory conditioning learning and long-term memory (Fig. 1A–C). These results agree with previous studies in the *Drosophila* FXS model[7,8], the mouse FXS model[62,63], and in human FXS patients[64,65]. Serotonergic neuromodulation is a conserved cognitive mechanism in all three cases[17,22,66]. Among serotonin receptors, 5-HT$_{2A}$R signaling is recognized as an important modulator of learning acquisition and memory consolidation in mammals[21]. However, 5-HT$_{2A}$R roles in learning and memory had not been previously tested in *Drosophila*. Here, we find that *5-HT$_{2A}$R* knockdown impairs both behaviors (Fig. 1A–C). Elevating 5-HT levels by itself does not enhance performance outcomes, although serotonergic signaling is known to regulate *Drosophila* learning and memory[22]. In the *Drosophila* FXS model, the underlying MB circuit (Fig. 1D–E) shows defects in experience-dependent Kenyon cell structure and function[5,11,67] consistent with serotonergic impairments. Fully-mapped brain 3-dimensional neural circuit reconstruction[68] reveals MB-innervating serotonergic neurons (Fig. 1E) that are well positioned to control learning and memory behavior in this system. Note this study focuses on a specific brain circuit and behavior, so cannot capture the full complexity of the FXS disease condition, and that further work is needed to clarify precise molecular, cellular, and circuit serotonergic mechanisms underlying broader FXS effects.

Elevating serotonin levels—either by overexpressing the rate-limiting serotonin synthesis enzyme Trhn (Fig. 2) or by knockdown of the serotonin reuptake transporter SERT (Fig. 3)—restores FXS learning and memory performance to the control levels. Global (*UH1*-Gal4), neural (*elav*-Gal4), and glial (*repo*-Gal4) drivers produce comparable correction, which is surprising, but consistent with neurons and glia both using Trhn and SERT to regulate serotonin levels[30,34]. Similar serotonergic-based effects occur in the mouse FXS model, although direct parallels must be interpreted cautiously, as serotonin receptor distributions and circuit functions differ between models. Specifically, mice with psilocybin can ameliorate cognitive deficits in *Fmr1* knockout mice[62]. SSRI treatments (e.g. sertraline) can likewise improve cognitive function in FXS children[69], supporting a conserved role for 5-HT elevation correcting FXS-related impairments. In the *Drosophila* FXS model, 5-HT levels are not altered in the MB learning/memory circuit, but Trhn overexpression and SERT knockdown elevate 5-HT in *dfmr1* nulls (Figs. 2, 3). Basal 5-HT levels are similar in the controls and *dfmr1* nulls, but increasing 5-HT levels is sufficient to activate the reduced number of 5-HT$_{2A}$Rs present in the FXS model. Thus, the defect is not a loss of serotonin itself, but rather reduced 5-HT$_{2A}$R abundance, and the behavioral deficits appear to arise from insufficient receptor availability rather than loss of ligand. Parallel findings in neural and glial drivers agree with Trhn and SERT in both cell types controlling serotonin levels[30]. Additional *Drosophila* glial mechanisms (e.g. arylalkylamine N-acetyltransferase 1) can also modulate 5-HT levels[70]. Mammalian glia also control serotonin homeostasis and signaling[71,72]. Our results indicate that raising 5-HT to levels very substantially above baseline via neuronal or glial mechanisms restores learning/memory behavior in the *Drosophila* FXS model, although whether this finding is generalizable remains to be determined.

Comparing these two strategies for increasing serotonin availability shows both restore learning and memory in the FXS model (Fig. 4A,B). This behavioral correction consistency suggests both methods converge on a shared outcome of higher 5-HT ligand levels, rather than targeting separable steps within the serotonergic regulatory pathway[73]. Our results argue against SERT being a principal site of FMRP action, for example, since reducing SERT does not yield different behavioral outcomes compared to Trhn overexpression. Blocking SERT using SSRIs is reportedly effective in cognitive preclinical trials[74,75]. Similarly, increasing serotonin via dietary tryptophan supplementation reportedly improves memory in cognitively impaired patients[76,77]. Elevating 5-HT has been suggested to compensate for 5-HT receptor loss to improve cognitive abilities[77]. Trhn overexpression is more effective than SERT knockdown in elevating serotonin levels in the MB learning/memory circuit (Fig. 4C,D). The absence of a training-induced 5-HT change indicates behavioral phenotypes do not arise from acute serotonin modulation by conditioning, but rather reflect differences in baseline serotonergic tone that determine the system capacity to support learning and memory (Fig. 4C,D). Although olfactory conditioning T-maze training has no discernible effect on 5-HT levels, neuronal and glial drivers are equally effective, with a trend toward an additive effect occurring with the ubiquitous driver. This result is surprising, but consistent with neurons and glia both using Trhn and SERT for serotonin signaling[30,34]. Importantly, behavioral changes from elevating 5-HT are observed only in *dfmr1* mutants in our studies, indicating that these manipulations act to correct a deficit specific to the FXS model rather than producing a general enhancement of performance. These results prompted us to focus on the downstream 5-HT receptor mechanism in our FXS disease model.

5-HT$_{2A}$R knockdown impairs learning and memory (Fig. 1), but in *dfmr1* nulls has a minimal additional effect on learning and no significant additive effect on memory (Fig. 5A,B). The 5-HT$_{2A}$R role is within neurons, with no function in glia. These results indicate FXS model behavioral impairments are mediated primarily through lost neuronal 5-HT$_{2A}$R signaling. Previous *Drosophila* studies have shown 5-HT$_{2A}$R signaling regulates locomotion[78], metabolic activity[79], and synapse pruning[30,34], but no prior work assessed roles in learning or memory. However, mouse 5-HT$_{2A}$Rs are involved in synaptic plasticity in mechanisms underlying cognition[80–82]. Human 5-HT$_{2A}$Rs regulate cortical function linked to cognitive impairment across multiple psychiatric conditions[21,83]. In the *Drosophila* FXS model, there is a significant 5-HT$_{2A}$R loss in the MB circuit (Fig. 5C–E). Just like for the 5-HT ligand, T-maze olfactory conditioning training has no discernible effect on the 5-HT$_{2A}$R levels. Similarly, lack of training-dependent modulation of 5-HT$_{2A}$Rs supports a model of fixed baseline 5-HT$_{2A}$R level, rather than dynamic regulation during conditioning, determining the efficiency of serotonergic signaling required for associative learning. Both neuronal and glial drivers similarly knockdown 5-HT$_{2A}$Rs, consistent with receptors being present in both cell types[30,34]. This suggests a regulatory maintenance mechanism within the MB circuit[84]. Previous studies have shown 5-HT$_{2A}$Rs expressed in the MB circuit[53], but this work now connects 5-HT$_{2A}$R signaling to learning/memory or FXS model behavioral dysfunction.

5-HT$_{2A}$R overexpression in *dfmr1* nulls is sufficient to restore learning and memory in our FXS disease model (Fig. 6A,B), which strongly reinforces the conclusion that serotonergic 5-HT$_{2A}$R signaling corrects behavioral impairments. 5-HT$_{2A}$Rs act primarily in neurons, but glial signaling also contributes, again suggesting balanced circuit-level modulation of receptor function[30]. We previously discovered glial *5-HT$_{2A}$R* overexpression allows experience-dependent synaptic connectivity remodeling[34], but there are no other studies of 5-HT$_{2A}$R overexpression in *Drosophila*. However, *5-HT$_{2A}$R* overexpression in *5-HT$_{2A}$R* knockout mice medial dorsal thalamus restores associative memory, demonstrating that enhancing 5-HT$_{2A}$R function can directly rescue cognitive deficits in mammals[85]. Pharmacological activation of 5-HT$_{2A}$Rs using agonists including 2,5-dimethoxy-4-iodoamphetamine (DOI), psilocybin, and LSD has been shown to promote neuroplasticity and 'cognitive flexibility', supporting potential applications for treating cognitive impairments[86–88]. In the *Drosophila* MB learning/memory circuit, 5-HT$_{2A}$R levels are independently confirmed as reduced in the FXS disease model and also elevated by transgenic overexpression in the *dfmr1* null mutants (Fig. 6C–E). 5-HT$_{2A}$R levels are elevated in all three of the transgenic drivers, with no significant differences comparing the untrained and associatively trained animals. These findings are consistent with a 5-HT$_{2A}$ receptor-limited mechanism, in which the reduced 5-HT$_{2A}$R level in *dfmr1* null mutants constrains serotonergic signaling within the learning/memory circuit, with highly elevated 5-HT levels overcoming the receptor deficit. These abnormally high 5-HT

levels could conceivably induce neurotrophic or plasticity-promoting factors to artificially drive correction of learning and memory impairments in our FXS model.

In *Fmr1* knockout mice, abnormal 5-HT_{2A} receptor function occurs in cortical circuits[36], and pharmacological 5-HT_{2A}R blockade ameliorates learning deficits[89]. However, serotonergic receptor distribution, downstream signaling, and circuit architectures differ substantially between mice and *Drosophila*. Thus, while both FXS models reveal 5-HT_{2A}R signaling disrupted by FMRP loss, the consequences and directionality of disruption depend on species-specific circuit contexts. Thus, our results define a 5-HT_{2A}R signaling role in the *Drosophila* FXS model, and do not contradict the distinct 5-HT receptor phenotypes observed in mice. Besides 5-HT_{2A}R, both 5-HT_{1A} and 5-HT_{7} receptors are expressed in the *Drosophila* brain[90]. 5-HT_{1A}R activation has been shown to rescue mitochondrial malfunction and motor impairments in the *Drosophila* FXS model[91], indicating that multiple 5-HT receptors are affected. Importantly, 5-HT_{7}R signaling plays a role in olfactory associative learning, with MB 5-HT_{7}Rs mediating cAMP-dependent learning[92]. Our work identifies 5-HT_{2A}R loss in the *Drosophila* FXS model MB circuit, but other 5-HT receptors could participate in the 5-HT_{2A}R-mediated effect on learning and memory. Since 5-HT ligand levels are unchanged in *dfmr1* mutants, and because behavioral restoration aligns precisely with manipulations that compensate for reduced 5-HT_{2A}R signaling, the simplest interpretation is that learning/memory impairments in this aversive conditioning task arise from insufficient 5-HT_{2A}R-mediated signaling. Thus, although 5-HT_{1A} and 5-HT_{7} receptors likely contribute to serotonergic functions in disease contexts, the combined molecular and behavioral evidence presented here identifies 5-HT_{2A}R as the key receptor mediating FXS-related deficits in MB-dependent learning and memory.

In conclusion, this investigation demonstrates that elevated serotonergic signaling corrects learning and memory impairments in the *Drosophila* Fragile X syndrome model. By transgenically increasing the 5-HT ligand levels (*Trhn* overexpression synthesis, *SERT* knockdown blocking uptake), serotonin is elevated to overcome a 5-HT_{2A}R limitation in the MB learning/memory circuit with learning and memory behavior restored in *dfmr1* nulls.

These findings support a baseline-tone mechanism, with learning and memory capacity determined by sufficient 5-HT_{2A}R levels, not dynamic signaling effects, acting to limit the signaling capacity rather than direct circuit plasticity in response to training. In future work, 5-HT_{2A}Rs could be selectively manipulated in defined serotonergic neurons (e.g. DPMs), using transgenic drivers to target the specific cells determining the serotonergic receptor-mediated signaling capacity. Importantly, 5-HT_{2A}Rs are downregulated in our FXS model, *5-HT_{2A}R* knockdown alone phenocopies *dfmr1* null mutant behavioral impairments, and *5-HT_{2A}R* knockdown in the FXS disease model only slightly exacerbates learning and memory deficits. These discoveries indicate that 5-HT_{2A}R signaling dysfunction appears causative in FXS disease model behavioral impairments. In future work, systemic use of SSRIs and 5-HT_{2A}R agonists could be attempted to assess whether the pharmacological activation of serotonergic signaling is sufficient to ameliorate learning and/or memory deficits in *dfmr1* mutants. Finally, inducing *5-HT_{2A}R* overexpression in our FXS disease model elevates receptor levels in the MB learning/memory circuit and corrects behavioral impairments in *dfmr1* mutants. These findings suggest serotonergic 5-HT_{2A}R signaling may be a useful means for FXS intervention strategies, pending future investigation in mammalian systems, and could provide a basis for future FXS therapeutic treatments.

Data availability

All original data analyzed during this study are publicly available within the Harvard Dataverse under the "Kendal Broadie Dataverse" heading. [https://dataverse.harvard.edu/dataverse/kendalbroadie].

Received: 19 September 2025; Accepted: 29 December 2025
Published online: 07 January 2026

References

1. Flavell, J., Franklin, C. & Nestor, P. J. A systematic review of fragile X-associated neuropsychiatric disorders. *JNP* **35**, 110–120 (2023).
2. Genovese, A. C. & Butler, M. G. Systematic review: Fragile X syndrome across the lifespan with a focus on genetics, neurodevelopmental, behavioral and psychiatric associations. *Genes (Basel)* **16**, 149 (2025).
3. Pieretti, M. et al. Absence of expression of the FMR-1 gene in Fragile X syndrome. *Cell* **66**, 817–822 (1991).
4. Verkerk, A. J. et al. Identification of a gene (FMR-1) containing a CGG repeat coincident with a breakpoint cluster region exhibiting length variation in Fragile X syndrome. *Cell* **65**, 905–914 (1991).
5. Sears, J. C. & Broadie, K. Use-dependent, untapped dual kinase signaling localized in brain learning circuitry. *J Neurosci* **44**, e1126232024 (2024).
6. Zhang, Y. Q. et al. *Drosophila* fragile X-related gene regulates the MAP1B homolog Futsch to control synaptic structure and function. *Cell* **107**, 591–603 (2001).
7. Bolduc, F. V., Bell, K., Cox, H., Broadie, K. & Tully, T. Excess protein synthesis is *Drosophila* Fragile X mutants impairs long-term memory. *Nat Neurosci* **11**(10), 1143–1145 (2008).
8. Jiang, H. et al. A fully automated *Drosophila* olfactory classical conditioning and testing system for behavioral learning and memory assessment. *J. Neurosci. Methods* **261**, 62–74 (2016).
9. Doll, C. A. & Broadie, K. Activity-dependent FMRP requirements in development of the neural circuitry of learning and memory. *Development* **142**, 1346–1356 (2015).
10. Pan, L., Zhang, Y. Q., Woodruff, E. & Broadie, K. The *Drosophila* fragile X gene negatively regulates neuronal elaboration and synaptic differentiation. *Curr. Biol.* **14**, 1863–1870 (2004).
11. Golovin, R. M., Vest, J. & Broadie, K. Neuron-specific FMRP roles in experience-dependent remodeling of olfactory brain innervation during an early-life critical period. *J. Neurosci.* **41**, 1218–1241 (2021).
12. Leahy, S. N., Song, C., Vita, D. J. & Broadie, K. FMRP activity and control of Csw/SHP2 translation regulate MAPK-dependent synaptic transmission. *PLoS Biol* **21**, e3001969 (2023).
13. Sears, J. C., Choi, W. J. & Broadie, K. Fragile X Mental Retardation Protein positively regulates PKA anchor Rugose and PKA activity to control actin assembly in learning/memory circuitry. *Neurobiol. Dis.* **127**, 53–64 (2019).

14. Davis, J. K. & Broadie, K. Multifarious functions of the fragile X mental retardation protein. *Trends Genet* **33**, 703–714 (2017).
15. Cea-Del Rio, C. A. et al. Disrupted inhibitory plasticity and homeostasis in Fragile X syndrome. *Neurobiol Dis* **142**, 104959 (2020).
16. Zhang, Y. Q. & Broadie, K. Fathoming Fragile X in fruit flies. *Trends Genet* **21**, 37–45 (2005).
17. Ciranna, L. & Costa, L. Therapeutic effects of pharmacological modulation of serotonin brain system in human patients and animal models of fragile X syndrome. *Int. J. Mol. Sci.* **26**, 2495 (2025).
18. Hanson, A. C. & Hagerman, R. J. Serotonin dysregulation in fragile X syndrome: Implications for treatment. *Intractable Rare Dis. Res.* **3**, 110–117 (2014).
19. Fernandez, S. P. et al. Constitutive and acquired serotonin deficiency alters memory and hippocampal synaptic plasticity. *Neuropsychopharmacology* **42**, 512–523 (2017).
20. Tortora, F. et al. The role of serotonin in fear learning and memory: A systematic review of human studies. *Brain Sci.* **13**, 1197 (2023).
21. Zhang, G. & Stackman, R. W. The role of serotonin 5-HT2A receptors in memory and cognition. *Front. Pharmacol.* **6**, 225 (2015).
22. Johnson, O., Becnel, J. & Nichols, C. D. Serotonin receptor activity is necessary for olfactory learning and memory in *Drosophila melanogaster*. *Neuroscience* **192**, 372–381 (2011).
23. Pooryasin, A. & Fiala, A. Identified serotonin-releasing neurons induce behavioral quiescence and suppress mating in *Drosophila*. *J. Neurosci.* **35**, 12792–12812 (2015).
24. de Belle, J. S. & Heisenberg, M. Associative odor learning in *Drosophila* abolished by chemical ablation of mushroom bodies. *Science* **263**, 692–695 (1994).
25. McGuire, S. E., Le, P. T. & Davis, R. L. The role of *Drosophila* mushroom body signaling in olfactory memory. *Science* **293**, 1330–1333 (2001).
26. Coates, K. E. et al. Identified serotonergic modulatory neurons have heterogeneous synaptic connectivity within the olfactory system of *Drosophila*. *J. Neurosci.* **37**, 7318–7331 (2017).
27. Lee, P.-T. et al. Serotonin-mushroom body circuit modulating the formation of anesthesia-resistant memory in *Drosophila*. *Proc. Natl. Acad. Sci. U. S. A.* **108**, 13794–13799 (2011).
28. Pech, U., Pooryasin, A., Birman, S. & Fiala, A. Localization of the contacts between Kenyon cells and aminergic neurons in the *Drosophila* melanogaster brain using SplitGFP reconstitution. *J. Comp. Neurol.* **521**, 3992–4026 (2013).
29. Sitaraman, D., LaFerriere, H., Birman, S. & Zars, T. Serotonin is critical for rewarded olfactory short-term memory in *Drosophila*. *J. Neurogenet.* **26**, 238–244 (2012).
30. Miller, V. K. & Broadie, K. Experience-dependent serotonergic signaling in glia regulates targeted synapse elimination. *PLoS Biol.* **22**, e3002822 (2024).
31. Greiss Hess, L. et al. A randomized, double-blind, placebo-controlled trial of low-dose sertraline in young children with fragile X syndrome. *J. Dev. Behav. Pediatr.* **37**, 619–628 (2016).
32. Indah Winarni, T. et al. Sertraline may improve language developmental trajectory in young children with fragile x syndrome: A retrospective chart review. *Autism Res. Treat.* **2012**, 104317 (2012).
33. Zhang, G. et al. Examination of the hippocampal contribution to serotonin 5-HT2A receptor-mediated facilitation of object memory in C57BL/6J mice. *Neuropharmacology* **109**, 332–340 (2016).
34. Miller, V. K. & Broadie, K. Glia-to-glia serotonin signaling directs MMP-dependent infiltration for experience-dependent synapse pruning. *PLoS Biol.* **23**, e3003524 (2025).
35. Liu, X., Kumar, V., Tsai, N.-P. & Auerbach, B. D. Hyperexcitability and homeostasis in fragile X syndrome. *Front. Mol. Neurosci.* **14**, 805929 (2021).
36. Xu, Z. H. et al. Deficits in LTP induction by 5-HT2A receptor antagonist in a mouse model for fragile X syndrome. *PLoS ONE* **7**(10), e48741 (2012).
37. Song, C. & Broadie, K. Fragile X mental retardation protein coordinates neuron-to-glia communication for clearance of developmentally transient brain neurons. *Proc. Natl. Acad. Sci. U. S. A.* **120**, e2216887120 (2023).
38. Jafar-Nejad, H., Tien, A.-C., Acar, M. & Bellen, H. J. Senseless and Daughterless confer neuronal identity to epithelial cells in the *Drosophila* wing margin. *Development* **133**, 1683–1692 (2006).
39. Sanfilippo, P., Smibert, P., Duan, H. & Lai, E. C. Neural specificity of the RNA-binding protein Elav is achieved by post-transcriptional repression in non-neural tissues. *Development* **143**, 4474–4485 (2016).
40. Halter, D. A. et al. The homeobox gene repo is required for the differentiation and maintenance of glia function in the embryonic nervous system of *Drosophila melanogaster*. *Development* **121**, 317–332 (1995).
41. Zeng, J. et al. Local 5-HT signaling bi-directionally regulates the coincidence time window for associative learning. *Neuron* **111**, 1118-1135.e5 (2023).
42. Shankar, S. et al. The neuropeptide tachykinin is essential for pheromone detection in a gustatory neural circuit. *Elife* **4**, e06914 (2015).
43. Gowda, S. B. M., Banu, A., Salim, S., Peker, K. A. & Mohammad, F. Serotonin distinctly controls behavioral states in restrained and freely moving *Drosophila*. *iScience* **26**, 105886 (2023).
44. Tully, T. & Quinn, W. G. Classical conditioning and retention in normal and mutant *Drosophila melanogaster*. *J. Comp. Physiol. A* **157**, 263–277 (1985).
45. Heisenberg, M. What do the mushroom bodies do for the insect brain? an introduction. *Learn. Mem.* **5**, 1–10 (1998).
46. Ganguly, I., Heckman, E. L., Litwin-Kumar, A., Clowney, E. J. & Behnia, R. Diversity of visual inputs to Kenyon cells of the *Drosophila* mushroom body. *Nat. Commun.* **15**, 5698 (2024).
47. Crittenden, J. R., Skoulakis, E. M., Han, K. A., Kalderon, D. & Davis, R. L. Tripartite mushroom body architecture revealed by antigenic markers. *Learn. Mem.* **5**, 38–51 (1998).
48. Hancock, C. E. et al. Visualization of learning-induced synaptic plasticity in output neurons of the *Drosophila* mushroom body γ-lobe. *Sci. Rep.* **12**, 10421 (2022).
49. Huang, C., Wang, P., Xie, Z., Wang, L. & Zhong, Y. The differential requirement of mushroom body α/β subdivisions in long-term memory retrieval in *Drosophila*. *Protein Cell* **4**, 512–519 (2013).
50. Yang, C.-H. et al. Additive expression of consolidated memory through *Drosophila* mushroom body subsets. *PLoS Genet* **12**, e1006061 (2016).
51. Lai, Y.-W. et al. Hormone-controlled changes in the differentiation state of post-mitotic neurons. *Curr. Biol.* **32**, 2341-2348.e3 (2022).
52. Dorkenwald, S. et al. Neuronal wiring diagram of an adult brain. *Nature* **634**, 124–138 (2024).
53. Lee, W.-P. et al. Serotonin signals modulate mushroom body output neurons for sustaining water-reward long-term memory in *Drosophila*. *Front. Cell Dev. Biol.* **9**, 755574 (2021).
54. Kuhn, D. M. & Hasegawa, H. Chapter 12 - Tryptophan hydroxylase and serotonin synthesis regulation. In *Handbook of Behavioral Neuroscience* (eds Müller, C. P. & Cunningham, K. A.) 239–256 (Elsevier, 2020).
55. Hu, S. W., Yang, Y. T., Sun, Y., Zhan, Y. P. & Zhu, Y. Serotonin signals overcome loser mentality in *Drosophila*. *iScience* **23**, 101651 (2020).
56. Knapp, E. M. et al. Mutation of the *Drosophila* melanogaster serotonin transporter dSERT impacts sleep, courtship, and feeding behaviors. *PLoS Genet* **18**, e1010289 (2022).
57. Kim, Y. et al. Pirenperone relieves the symptoms of fragile X syndrome in Fmr1 knockout mice. *Sci. Rep.* **12**, 20966 (2022).

58. Richter, J. D. & Zhao, X. The molecular biology of FMRP: New insights into fragile X syndrome. *Nat. Rev. Neurosci.* **22**, 209–222 (2021).
59. Sears, J. C. & Broadie, K. Fragile X mental retardation protein regulates activity-dependent membrane trafficking and trans-synaptic signaling mediating synaptic remodeling. *Front. Mol. Neurosci.* **10**, 440 (2017).
60. Li, Y.-J. et al. Improvement of learning and memory by elevating brain D-aspartate in a mouse model of fragile X syndrome. *Mol. Neurobiol.* **60**, 6410–6423 (2023).
61. Sears, J. C. & Broadie, K. FMRP-PKA activity negative feedback regulates RNA binding-dependent fibrillation in brain learning and memory circuitry. *Cell Rep.* **33**, 108266 (2020).
62. Buzzelli, V. et al. Psilocybin mitigates the cognitive deficits observed in a rat model of fragile X syndrome. *Psychopharmacology* **240**, 137–147 (2023).
63. Willemsen, R. & Kooy, R. F. Mouse models of fragile X-related disorders. *Dis. Model. Mech.* **16**, dmm049485 (2023).
64. Bostrom, C. et al. Hippocampal dysfunction and cognitive impairment in fragile-X syndrome. *Neurosci. Biobehav. Rev.* **68**, 563–574 (2016).
65. Chen, Y.-S. et al. Early 7,8-dihydroxyflavone administration ameliorates synaptic and behavioral deficits in the young FXS animal model by acting on BDNF-TrkB pathway. *Mol. Neurobiol.* **60**, 2539–2552 (2023).
66. Coray, R. & Quednow, B. B. The role of serotonin in declarative memory: A systematic review of animal and human research. *Neurosci. Biobehav. Rev.* **139**, 104729 (2022).
67. Doll, C. A. & Broadie, K. Neuron class-specific requirements for fragile X mental retardation protein in critical period development of calcium signaling in learning and memory circuitry. *Neurobiol. Dis.* **89**, 76–87 (2016).
68. Robinson, J. W. et al. The *Drosophila* adult brain: Short overview of structure, function, and resources graphical review paper. *Curr. Res. Insect Sci.* **7**, 100113 (2025).
69. AlOlaby, R. R. et al. Molecular biomarkers predictive of sertraline treatment response in young children with fragile X syndrome. *Brain Dev.* **39**, 483–492 (2017).
70. Davla, S. et al. AANAT1 functions in astrocytes to regulate sleep homeostasis. *Elife* **9**, e53994 (2020).
71. Allen, N. J. & Lyons, D. A. Glia as architects of central nervous system formation and function. *Science* **362**, 181–185 (2018).
72. Lines, J., Corkrum, M., Aguilar, J. & Araque, A. The duality of astrocyte neuromodulation: Astrocytes sense neuromodulators and are neuromodulators. *J. Neurochem.* **169**, e70054 (2025).
73. Jones, L. A., Sun, E. W., Martin, A. M. & Keating, D. J. The ever-changing roles of serotonin. *Int. J. Biochem. Cell Biol.* **125**, 105776 (2020).
74. Tahiri, J. et al. Serotonin in depression and Alzheimer's disease: Focus on SSRI's beneficial effects. *Ageing Res. Rev.* **101**, 102537 (2024).
75. Wang, H. et al. Efficacy of selective serotonin reuptake inhibitors-related antidepressants in Alzheimer's disease: a meta-analysis. *Eur. J. Med. Res.* **29**, 438 (2024).
76. Jenkins, T. A., Nguyen, J. C. D., Polglaze, K. E. & Bertrand, P. P. Influence of tryptophan and serotonin on mood and cognition with a possible role of the gut-brain axis. *Nutrients* **8**, 56 (2016).
77. Mohajeri, M. H. et al. Chronic treatment with a tryptophan-rich protein hydrolysate improves emotional processing, mental energy levels and reaction time in middle-aged women. *Br. J. Nutr.* **113**, 350–365 (2015).
78. Park, J., Kondo, S., Tanimoto, H., Kohsaka, H. & Nose, A. Data-driven analysis of motor activity implicates 5-HT2A neurons in backward locomotion of larval *Drosophila*. *Sci. Rep.* **8**, 10307 (2018).
79. Lyu, Y. et al. *Drosophila* serotonin 2A receptor signaling coordinates central metabolic processes to modulate aging in response to nutrient choice. *Elife* **10**, e59399 (2021).
80. Berthoux, C., Barre, A., Bockaert, J., Marin, P. & Bécamel, C. Sustained Activation of postsynaptic 5-HT2A receptors gates plasticity at prefrontal cortex synapses. *Cereb Cortex* **29**, 1659–1669 (2019).
81. Desrochers, S. S. & Nautiyal, K. M. Serotonin 1B receptor effects on response inhibition are independent of inhibitory learning. *Neurobiol. Learn. Mem.* **187**, 107574 (2022).
82. Grieco, S. F. et al. Psychedelics and neural plasticity: therapeutic implications. *J. Neurosci.* **42**, 8439–8449 (2022).
83. Luppi, A. I. et al. A role for the serotonin 2A receptor in the expansion and functioning of human transmodal cortex. *Brain* **147**, 56–80 (2024).
84. Lee, J.-E. et al. The role of glial and neuronal Eph/ephrin signaling in *Drosophila* mushroom body development and sleep and circadian behavior. *Biochem. Biophys. Res. Commun.* **720**, 150072 (2024).
85. Barre, A. et al. Presynaptic serotonin 2A receptors modulate thalamocortical plasticity and associative learning. *Proc. Natl. Acad. Sci.* **113**, E1382–E1391 (2016).
86. Bedford, P. et al. The effect of lysergic acid diethylamide (LSD) on whole-brain functional and effective connectivity. *Neuropsychopharmacology* **48**, 1175–1183 (2023).
87. Meshkat, S. et al. Impact of psilocybin on cognitive function: A systematic review. *Psychiatry Clin. Neurosci.* **78**, 744–764 (2024).
88. Šabanović, M. et al. Lasting dynamic effects of the psychedelic 2,5-dimethoxy-4-iodoamphetamine ((±)-DOI) on cognitive flexibility. *Mol. Psychiatry* **29**, 1810–1823 (2024).
89. Lim, C. S. et al. Pharmacological rescue of Ras signaling, GluA1-dependent synaptic plasticity, and learning deficits in a fragile X model. *Genes. Dev.* **28**(3), 273–289 (2014).
90. Silva, B., Goles, N. I., Varas, R. & Campusano, J. M. Serotonin receptors expressed in Drosophila mushroom bodies differentially modulate larval locomotion. *PLoS ONE* **9**(2), e89641 (2014).
91. Vannelli, A., Mariano, V., Bagni, C. & Kanellopoulos, A. K. Activation of the 5-HT1A receptor by eltoprazine restores mitochondrial and motor deficits in a drosophila model of fragile X syndrome. *Int. J. Mol. Sci.* **25**(16), 8787 (2024).
92. Ganguly, A., Qi, C., Bajaj, J. & Lee, D. Serotonin receptor 5-HT7 in Drosophila mushroom body neurons mediates larval appetitive olfactory learning. *Sci. Rep.* **10**(1), 21267 (2020).

Acknowledgements

We are grateful to the Bloomington Drosophila Stock Center (BDSC; Indiana University, Bloomington, IN, USA) for essential genetic stocks, and to the Developmental Studies Hybridoma Bank (DSHB; University of Iowa, Iowa City, IA, USA) for essential antibodies. We thank Broadie Lab members for extensive and insightful input throughout this study.

Author contributions

Conceptualization: K.B., V.M.; Methodology: Y.D., V.M., A.M.; Validation: Y.D., A.M.; Formal analyses: Y.D., A.M.; Investigation: Y.D.; Data curation: Y.D.; Visualization: Y.D.; Writing—original draft: Y.D.; Writing—review and editing: K.B., Y.D.; Resources: K.B.; Supervision: V.M., K.B.; Administration: K.B.; Funding: K.B.

Funding

This work is funded by National Institute of Health grants R01 NS131557 and NS13287 to K.B.

Declarations

Competing interests
The authors declare no competing interests.

Additional information
Supplementary Information The online version contains supplementary material available at https://doi.org/10.1038/s41598-025-34492-4.

Correspondence and requests for materials should be addressed to K.B.

Reprints and permissions information is available at www.nature.com/reprints.

Publisher's note Springer Nature remains neutral with regard to jurisdictional claims in published maps and institutional affiliations.